Table 2
ID_{50} of heparin and three derivatives against infection of VSV based-pseudotyped viruses carrying Env of MLV into NIH 3T3 cells.

Reagents	VSV based-pseudotyped viruses		
	VSV/F-Env	VSV/A8-Env	VSV/PVC-211-Env
Heparin	7.0 ± 0.3[a]	8.0 ± 0.3[a]	7.4 ± 0.4[a]
NAdOS-H	>1000	>1000	>1000
NA-H	50.1 ± 3.9	53.4 ± 2.6	50.8 ± 3.7
dNS-H	67.8 ± 1.5	64.8 ± 2.0	71.5 ± 1.8

ID_{50} values (μg/ml) were calculated from the data shown in Fig. 3. The mean values (and SEMs) of 4 independent experiments are shown. Statistical comparison was performed using the *t* test. NAdOS-H: *N*-acetyl-de-*O*-sulfated heparin; NA-H:*N*-acetyl-heparin; dNS-H: de-*N*-sulfated heparin.

[a] $P<0.001$ vs NA-H and dNS-H in each virus.

Effect of polybrene on heparin-induced inhibition of MLV infection

In order to determine the effect of polybrene on the inhibitory activity of heparin against MLV infection, we performed experiments in the presence and absence of polybrene. Firstly, we examined the effects of polybrene on MLV infection at an MOI of 1. In the absence of polybrene, at 72 h post-infection, viral production of MLVs was undetectable level by an RT assay; at 96 h post-infection, viral production was detectable but was 10- to 50-fold lower than in the presence of polybrene (data not shown). In the presence of polybrene, viral production at 96 h post-infection was higher than at 72 h post-infection. Therefore, we evaluated viral production at 96 h post-infection in the following experiment. F-, A8, and PVC-211 MLVs were pre-incubated with various concentrations of heparin in the absence of polybrene, and then inoculated onto NIH 3T3 cells at an MOI of 1 either in the presence of 10 μg/ml polybrene or in its absence; viral production was evaluated at 96 h. In the presence of polybrene, the ID_{50} values of heparin for F-, A8, and PVC-211 MLVs were 44.4 ± 6.7, 47.9 ± 0.8, and 49.6 ± 2.2 μg/ml, respectively; these values were not significantly different (Fig. 5A and Table 3). The ID_{50} values in this experiment are higher than those shown in Fig. 1A and Table 1 due to differences in culture time; nevertheless, the inhibition curves in Fig. 5A are similar to those in Fig. 1A. In the absence of polybrene, the ID_{50} values of heparin for F-, A8, and PVC-211 MLVs were 0.56 ± 0.08, 0.61 ± 0.10, and 0.60 ± 0.05 μg/ml, respectively (Fig. 5B and Table 3); these values are not significantly different. However, these values are significantly lower than those in the presence of polybrene ($P<0.001$).

We also attempted to examine the effects of polybrene on the inhibitory activity of heparin against infection of NIH 3T3 cells by VSV-pseudotyped viruses. However, the efficiency of GFP gene transduction of the cells with the pseudotyped viruses in the absence of polybrene was too low to allow the effects of heparin to be reliably compared (data not shown).

Discussion

Soluble GAGs, such as heparin, have been shown to inhibit infection by MLV (Guibinga et al., 2002; Jinno-Oue et al., 2001; Walker et al., 2002). It has been reported that this inhibitory effect is determined by a number of factors: GAG concentration; electrostatic charge on the GAG; the affinity of the virus to the GAG; the cells from which the viruses are produced; and the cell type infected with the viruses. In this study, we examined the effects of soluble GAGs on the ability of ecotropic MLVs produced by NIH 3T3 cells to infect NIH 3T3 cells. Jinno-Oue et al. (2001) showed that, in the absence of polybrene, low concentrations of heparin (up to 100 μg/ml) enhanced the infectivity of F- and PVC-211 MLVs, whereas higher concentrations inhibited infectivity. In contrast, we found that 0.1 μg/ml of heparin did not affect the infectivity of F-, A8, and PVC-211 MLVs in the absence of polybrene; however, concentrations greater than 1 μg/ml, heparin inhibited infectivity (Fig. 5B). In the presence of polybrene, we found that 1 μg/ml or less of heparin did not affect the infectivity of F-, A8, and PVC-211 MLVs; at concentrations greater than 10 μg/ml, however, heparin inhibited infectivity in a dose-dependent manner (Figs. 1A and 5A). The apparent lack of any enhancing effects of heparin on ecotropic MLV infectivity in the present study may be due to differences in experimental conditions. Thus, the discrepant results in this and the previous study might be a consequence of using different cell types in which to measure viral infectivities. Jinno-Oue et al. (2001) used Rat-1 and primary rat brain capillary endothelial cells (BCEC) as target cells, while we used mouse NIH 3T3 cells.

Walker et al. (2002) and Guibinga et al. (2002) reported that the cell surface attachment of Env-deficient retrovirus-like particles was inhibited by heparin, suggesting that heparin inhibits Env-independent interaction of MLV with target molecules on the cell surface. By contrast, Jinno-Oue et al. (2001) showed that subtle changes in the Env protein amino acid sequences, which generated a heparin-binding site(s), could affect the heparin-binding affinity of the viruses and the susceptibility of the viruses to the effects of heparin. Thus, it is likely that heparin influences not only Env-independent attachment, but also Env-dependent attachment of the virus to the cell surface. In our present study, the binding to heparin by VSV-based pseudotyped viruses carrying the Env of F-, A8, or PVC-211 MLVs was quantitatively examined by SPR analysis. To our knowledge, the present study is the first to quantitatively compare heparin binding activities of Env of different ecotropic MLVs using SPR technology. Our results indicated that the binding activities of VSV based-pseudotyped viruses carrying the Env of ecotropic MLVs were higher than that of the Env-deficient virus-like particle, and that the Env sequence influenced the binding activity of the pseudotyped viruses to heparin (Figs. 4 and 6). Therefore, the results strongly suggest that the Env per se of these ecotropic MLVs can directly interact with heparin. PVC-211-Env exhibited the highest heparin binding activity, followed by A8-Env, and then F-Env (Fig. 4). These results are consistent with those of a previous study in which heparin agarose was used to assess the heparin binding activities of F-MLV and PVC-211 MLV (Jinno-Oue et al., 2001). F-Env, which showed the lowest binding activity to heparin, had 26 amino acid substitutions compared to A8-Env (Fig. 6). By contrast, A8-Env and PVC-211-Env showed similar binding activities and differed by only 3 amino acids (Fig. 6). The consensus sequences for the heparin-binding domain (HBD) are XBBXBX and XBBBXXBX, where X represents any amino acid and B indicates a basic amino acid (Cardin and Weintraub, 1989). A stretch of 6 amino acids from Ser^{124} to Glu^{129} in the receptor-binding domain (RBD) of F-Env constitutes a putative HBD. However, a previous study suggested that this sequence did not function as an HBD (Jinno-Oue et al., 2001). Compared to F-Env, the substitution of Glu^{129} by Lys in PVC-211-Env generated an additional, overlapping HBD from Pro^{127} to Ser^{132}. This new HBD has been suggested to contribute to the high binding ability of PVC-211 MLV for heparin. Intriguingly, the amino acids at positions 124 to 132 of A8-Env are identical to those of F-Env, and thus A8-Env has only one putative HBD that might not be functional. Therefore, the number of HBDs cannot explain the difference in binding activities of A8-Env and F-Env to heparin. Recently, the heparin binding activities of wild-type and mutant gp120 of HIV-1 were studied using SPR-based binding assays (Crublet et al., 2008). Four new HBDs were identified in the V2 and V3 loops, in the C-terminal domain, and within the CD4-induced bridging sheet. Three of these HBDs were found in domains of the protein that are involved in co-receptor recognition. In particular, Arg^{419}, Lys^{421}, and Lys^{432}, which directly interact with the co-receptor, are targeted by heparin, suggesting that these basic amino acids are important for the interaction with heparin. In contrast to F-Env, which has Gln^{61} and Ser^{80} in the variable region A (VRA) of RBD, both A8-Env and PVC-211-Env have Arg^{61} and Arg^{80} in common (Fig. 6). Therefore, we suggest that

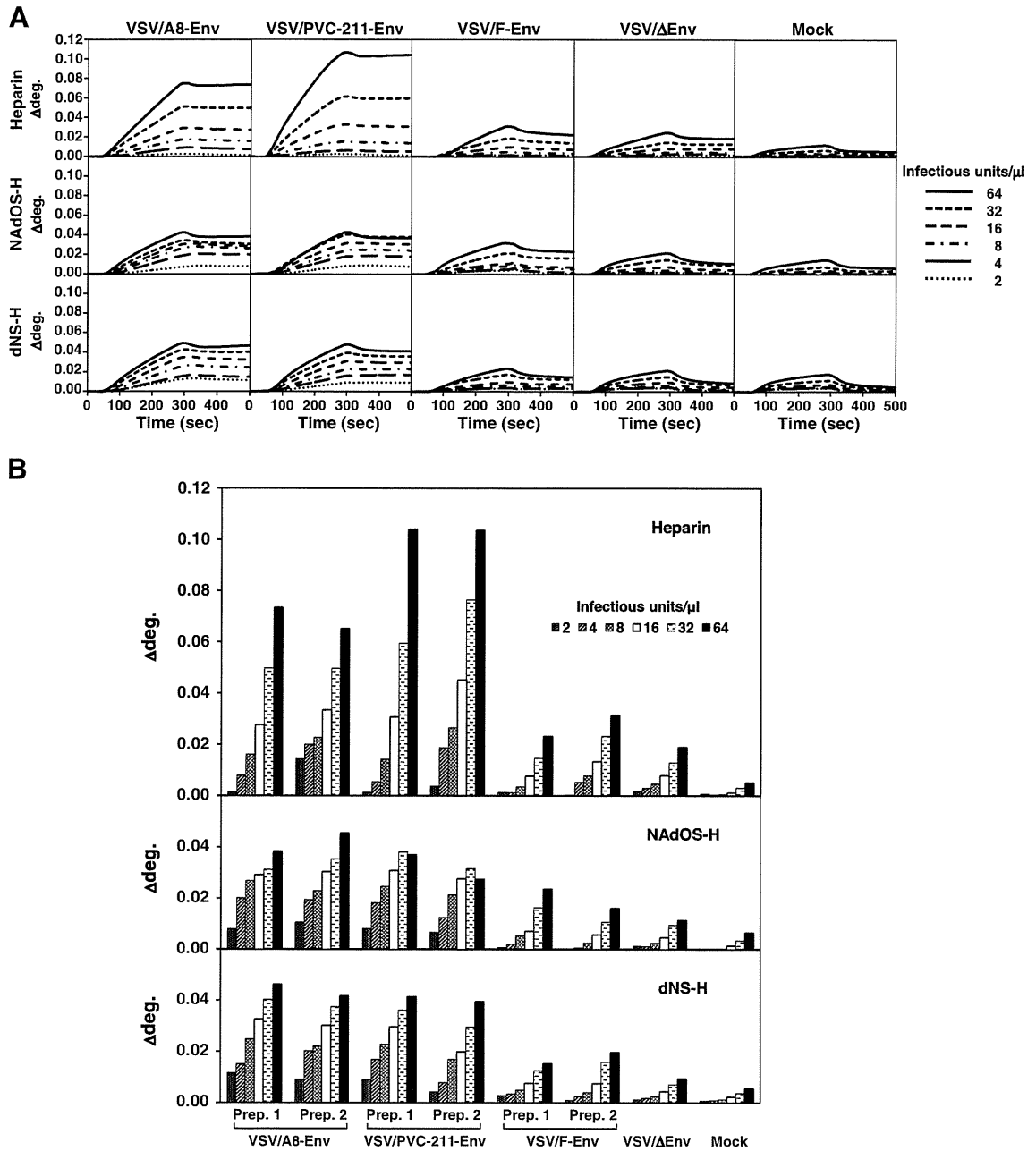

Fig. 4. SPR analysis of the binding of VSV based-pseudotyped viruses carrying Env of F- (VSV/F-Env), A8 (VSV/A8-Env), or PVC-211 MLV (VSV/PVC-211-Env) to heparin, NAdOS-H (*N*-acetyl-de-*O*-sulfated heparin), or dNS-H (de-*N*-sulfated heparin) immobilized on SPR sensor chips. Two independent preparations (Prep. 1 and Prep. 2) of VSV/F-Env, VSV/A8-Env, and VSV/PVC-211-Env were tested. (A) SPR sensorgrams of viral particles of Prep. 1 for the Heparin chip, the NAdOS-H chip, or the dNS-H chip. (B) The equilibrium level of binding of viral particles to the Heparin chip, the NAdOS-H chip, or the dNS-H chip at 450 s. VSV/ΔEnv: Env-deficient VSV-like particles; Mock: culture supernatants of 293T cells. 1×10^6 infectious units of VSV based-pseudotyped viruses carrying Env were prepared and treated for SPR analysis as described in the Materials and methods section. VSV/ΔEnv and Mock controls were prepared as described in the Materials and methods section. The aliquots from both controls were equivalent in volume to those from the culture supernatants of VSV/Env-producing cells, which contained 1×10^6 infectious units, and were treated in the same manner.

these two residues in A8- and PVC-211-Env might contribute to the higher heparin-binding activity. Furthermore, Lys^{129} is present only in PVC-211-Env and may be responsible for the additional heparin-binding activity.

Although PVC-211-Env had the highest heparin binding activity, followed by A8-Env, and then F-Env (Fig. 4), the ID_{50} values of heparin for infection by PVC-211, A8, or F-MLV were not significantly different (Fig. 1 and Table 1). Similarly, the ID_{50} values of heparin for infection of VSV-based pseudotyped viruses bearing PVC-211-, A8-, or F-Env were not significantly different (Fig. 3 and Table 2). The reasons why the estimates for inhibition of viral infection do not correlate with those from the SPR analyses are not clear, but the following possibilities could be suggested. First, the relatively low binding activity of Env to heparin, which was observed in the SPR analysis of F-Env, might be sufficient to block viral infection. Second, the SPR analysis might be more sensitive to heparin-binding activity than the inhibition assay of viral infectivity. In the SPR analysis, viral particles bind to heparin immobilized to a chip, and then excess and low-affinity viral particles are washed out. In contrast, in the inhibition assay, small soluble molecules of heparin bind to the Env of viruses, and thus relatively low-affinity binding between heparin and Env could have a significant effect on viral

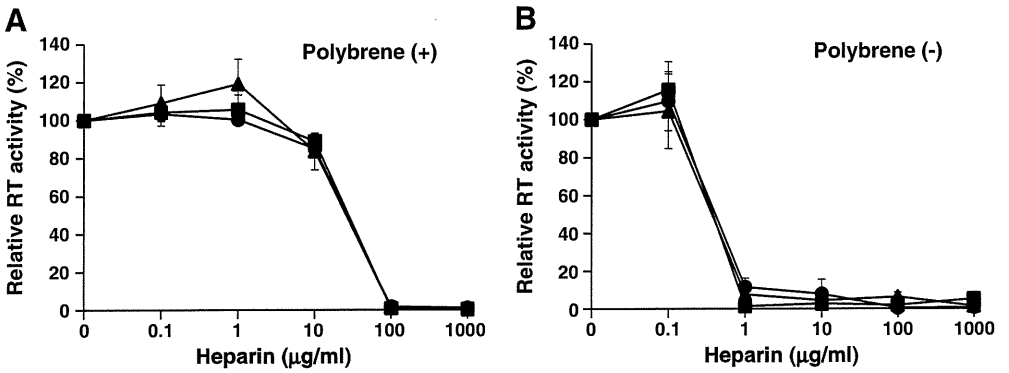

Fig. 5. Effects of polybrene on inhibitory activities of heparin against MLV infection. F- (triangle), A8 (circle), and PVC-211 (square) MLVs were pre-incubated with various concentrations of heparin for 1 h at 37 °C in the absence of polybrene. Then, the virus–heparin mixture was inoculated onto NIH 3T3 cells in the presence of 10 μg/ml polybrene (A) or in its absence (B). After incubation for 1 h at 37 °C, the cells were washed three times with FCS-free DMEM and fresh culture medium was added. After 96 h, virion-associated RT activity in the culture supernatants was measured by an RT assay as described in the Materials and methods section. The mean values of 4 independent experiments and SEM are shown.

infection. Third, we cannot exclude the possibility that heparin might affect viral replication steps except for attachment. Although we used VSV-pseudotyped viruses carrying Env for the inhibition assay against viral infection, the assay did not distinguish rigorously between viral attachment and alternative steps in infection, such as entry and gene expression. Therefore, heparin might not only influence viral attachment but also entry and gene expression, with the result that the ID_{50} values for viral infection are similar among the viruses despite the fact that they carry different Envs.

Heparin is a highly sulfated polysaccharide with a negative charge and its most common disaccharide unit is composed of 2-*O*-sulfated iduronic acid and 6-*O*-sulfated, *N*-sulfated glucosamine (Fig. 1E). Sulfation of heparan sulfate, which is structurally related to heparin, is thought to play an important role in its biological activity such as FGF signaling and its ability to act as an entry receptor for herpes simplex virus type 1 (Capila and Linhardt, 2002; Copeland et al., 2008; Shukla et al., 1999; Xia et al., 2002; Ye et al., 2001). It has also been shown that the chemical structure of the carbohydrate unit constituting the GAG backbone is an important determinant for the ability of the GAG to inhibit retroviral infection (Jinno-Oue et al., 2001; Walker et al., 2002). By comparing the effects of heparin and dNS-H, Jinno-Oue et al. (2001) concluded that *N*-sulfation of GAG is important for the effects on infectivity of ecotropic MLVs. In this study, NA-H, which has diminished *N*-sulfation, and dNS-H, which completely lacks *N*-sulfation, were shown to be less effective than heparin in inhibiting infection of NIH 3T3 cells by pseudotyped viruses carrying ecotropic MLV Env (Fig. 3 and Table 2). We have, therefore, confirmed that *N*-sulfation of GAG plays an important role in the inhibition of ecotropic MLV infection. In addition, NAdOS-H, which has markedly diminished *N*-sulfation and completely lacks *O*-sulfation, did not significantly alter infectivity of pseudotyped viruses on NIH 3T3 cells (Fig. 3). Comparison of dNS-H and NAdOS-H strongly suggests that the *O*-sulfate groups of GAG are also required for the inhibitory effects on MLV infection. Intriguingly, the results of the SPR analysis indicated that NAdOS-H, which failed to inhibit ecotropic MLV infection, binds to F-, A8-, and PVC-211-Env at levels comparable to those of dNS-H, which unequivocally exhibited inhibitory effects on viral infection. Therefore, binding of GAG to the viral Env may be essential, but not sufficient, for inhibition of Env-dependent MLV attachment to the cell surface. Previous studies have highlighted the importance of the *O*-sulfate group of heparin for its inhibitory activities against infection by pseudorabies virus (Trybala et al., 1996), herpes simplex virus (Trybala et al., 2000), and HIV (Rider et al., 1994). In contrast, *N*-sulfation of heparin is required for inhibition of respiratory syncytial virus infection (Hallak et al., 2000). The results from the

Table 3
ID_{50} of heparin against infection of MLVs into NIH 3T3 cells in the presence or absence of polybrene.

Polybrene	Viruses		
	F	A8	PVC-211
Present	44.4 ± 6.7	47.9 ± 0.8	49.6 ± 2.2
Absent	0.56 ± 0.08[a]	0.61 ± 0.10[a]	0.60 ± 0.05[a]

ID_{50} values (μg/ml) were calculated from the data shown in Fig. 5. The mean values (and SEMs) of 4 independent experiments are shown. Statistical comparison was performed using the t test.

[a] $P < 0.001$ vs presence of polybrene in each virus.

Position	Amino Acid F	A8	PVC-211	Structural element
-28	Pro	Ser	Ser	
1	Ala	Val	Ala	RBD
40	Val	Asp	Asp	RBD
61	Gln	Arg	Arg	RBD-VRA
79	Ser	Asn	Asn	RBD-VRA
80	Ser	Arg	Arg	RBD-VRA
84	Ser	Ser	Ala	RBD-VRA
116	Glu	Gly	Gly	RBD-VRA
129	Glu	Glu	Lys	RBD-VRC
152	Val	Ala	Ala	RBD
172	Ser	Asn	Asn	RBD-VRB
175	Val	Ala	Ala	RBD-VRB
203	Thr	Ile	Ile	RBD
216	Arg	Gln	Gln	RBD
227	Arg	Lys	Lys	RBD
249	Leu	Phe	Phe	
251	Arg	Leu	Leu	
263	Pro	Ser	Ser	
277	Thr	Ala	Ala	
319	Gly	Ala	Ala	
344	Val	Ala	Ala	
345	Ala	Gly	Gly	
358	Arg	Gln	Gln	
379	Ile	Thr	Thr	
380	Asp	Gly	Gly	
390	Thr	Ala	Ala	
393	Thr	Met	Met	
642	End	Gln	Gln	

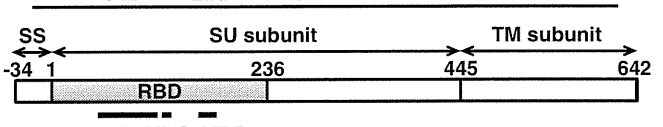

Fig. 6. Amino acid sequences of F-, A8-, and PVC-211-Env. A schematic diagram of the Env precursor polyprotein is shown at the bottom. SS: signal sequence; SU: surface protein; TM: transmembrane protein; RBD: receptor-binding domain (Fass et al., 1997); VRA: variable region A; VRB: variable region B; VRC: variable region C. The N-terminal amino acid of the SU is numbered as 1.

earlier studies and from here suggest that different types of sulfate groups are required for the inhibitory activities of heparin against different viruses, and that the anti-viral activity of heparin does not depend simply on negative charge density but involves particular structures, notably sulfation patterns.

Although the interaction between Env and CAT-1, the receptor molecule for MLV, appears to be required for membrane fusion and entry of the viral capsid, it has been reported that initial attachment of MLV to the cell surface can take place in a receptor-independent manner (Guibinga et al., 2002; Pizzato et al., 1999; Walker et al., 2002). Heparan sulfate on the cell surface was proposed as a candidate cell surface molecule for MLV attachment (Batra et al., 1997; Guibinga et al., 2002; Jinno-Oue et al., 2001; Le Doux et al., 1996, 1999; Masuda et al., 1997; Walker et al., 2002). The SPR analyses carried out in the present study also suggest that heparan sulfate on the cell surface is involved in MLV attachment as we found that heparin could bind directly to the Env of MLV. The exact role(s) of the cell surface heparan sulfate in MLV infection is still unknown; nevertheless,

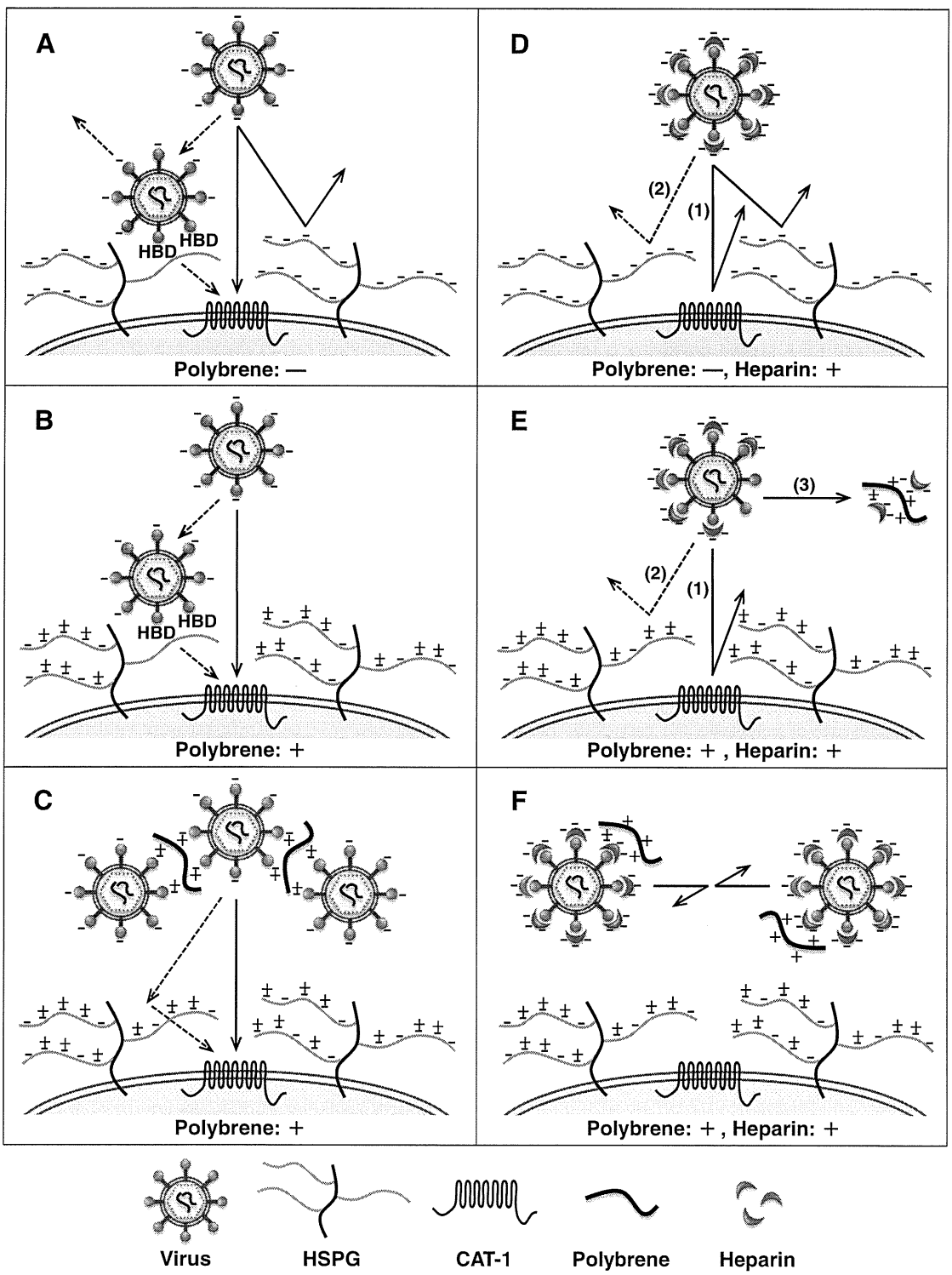

Fig. 7. Schematic diagrams of possible mechanisms of attachment of MLV to cells and of the inhibition of attachment by heparin. These various possibilities are described in detail in the Discussion section. CAT-1: cationic amino acid transporter 1 as the specific receptor for ecotropic MLV; HSPG: heparan sulfate proteoglycan.

we suggest a possible model for its behavior in Fig. 7. In this model, heparan sulfate on the cell surface is envisaged as a route for viral infection. The viral particles first bind to heparan sulfate via the HBD of Env and the increase in concentration of viral particles on the cell surface then raises the probability of interaction with CAT-1. On the cell surface, CAT-1 is covered by long chains of heparan sulfate that have a large net negative charge. In the absence of polybrene, it is difficult for viral particles with a negative charge to approach CAT-1 and/or heparan sulfate on the cell surface due to electrostatic repulsion (Fig. 7A). MLV infections are usually carried out in the presence of cationic polymers, such as polybrene to enhance infection, because the infectivity of MLV is very low in the absence of polybrene (Davis et al., 2002). Polybrene appears to enhance the infectivity of MLVs through various possible mechanisms, and some of these have been identified in previous studies. Initially, the positive charge of polybrene might neutralize the negative charge on the cell surface, facilitating access of the viral particles to CAT-1 and/or heparan sulfate on the cell surface (Fig. 7B) (Davis et al., 2004). A second possibility is that polybrene might cause the viral particles to form aggregates that have easier access to the cell surface (Fig. 7C) (Davis et al., 2004; Landazuri and Le Doux, 2004). Based on these putative mechanisms, how might heparin inhibit infection by ecotropic MLV? It is possible that heparin binds to a region near the RBD of Env and sterically or electrostatically blocks interaction between Env and CAT-1 (arrow (1) in Figs. 7D and E). A second possibility is that heparin binds to HBD of Env and that viral particles covered with heparin cannot bind to heparan sulfate on the cell surface (arrow (2) in Figs. 7D and E). Alternatively, viral particles bearing heparin have a large net negative charge and might fail to access the cell surface due to electrostatic repulsion. A final possibility is that polybrene might not be able to aggregate heparin-covered viral particles that bear large negative charges, and this might make access to the cell surface less efficient (Fig. 7F). The ID_{50} values of heparin for F-, A8, and PVC-211 MLVs were lower in the absence of polybrene than in its presence (Fig. 5 and Table 3). In the absence of polybrene, the negative charge of cell surface molecules is not neutralized. Therefore, it is possible that the repulsion between viral particles bearing heparin and cell surface molecules with a negative charge is stronger in the absence of polybrene than in its presence (Figs. 7D and E). As a result, heparin is able to inhibit viral infection effectively in the absence of polybrene. Alternatively, in the presence of polybrene, the part of the heparin molecule that normally binds to viral particles might instead bind with polybrene (arrow (3) in Fig. 7E), with the consequence that a relatively large amount of heparin is required for inhibition of viral infection.

Materials and methods

Reagents

Heparin (H4784), *N*-acetylheparin (A8036) (NA-H), de-*N*-sulfated heparin (D4776) (dNS-H), and *N*-acetyl-de-*O*-sulfated heparin (A6039) (NAdOS-H) were obtained from Sigma. Heparin obtained from Nacalai Tesque was used in the SPR analysis.

Cells and viruses

NIH 3T3 cells were grown in Dulbecco's modified Eagle's medium (DMEM) containing 10% fetal calf serum (FCS). *Mus dunni* cells were grown in RPMI1640 medium containing 10% FCS. 293T cells were grown on DMEM containing 5% FCS.

Infectious DNA clones of neuropathogenic A8 (Takase-Yoden and Watanabe, 1997; Watanabe and Takase-Yoden, 1995) (database ID: D88386) and PVC-211 MLVs (Kai and Furuta, 1984; Masuda et al., 1992) (database ID: M93134.1) and non-neuropathogenic F-MLV clone 57 (Oliff et al., 1980) (database ID: X02794) were described previously. NIH 3T3 cells were transfected with each DNA clone, and culture supernatants of the virus-producing cells were harvested and stored at −80 °C as stock viruses. Virus titers were determined by a focal immunoassay on *Mus dunni* cells in the presence of 10 μg/ml polybrene as described previously (Czub et al., 1991).

Assay of viral reverse transcriptase

Culture supernatants of the virus-producing cells were centrifuged at 5000 rpm for 5 min at 4 °C. To disrupt the viral particles, 10 μl of the supernatant was mixed with 14 μl of an aqueous solution of 7 mM Tris–HCl (pH7.6), 70 mM NaCl, 0.7 mM ethylenediaminetetraacetic acid (EDTA), and 0.03% Triton X-100. The mixture was then mixed with 16 μl of an aqueous solution of 125 mM Tris–HCl (pH7.6), 150 mM NaCl, 25 mM dithiothreitol, 2.5 mM $MnCl_2$, 250 μg/ml Poly(A) x $(dT)_{15}$ (Roche Diagnostics), and ^{3}H-TTP (1 μCi), and incubated for 1 h at 37 °C (Robert-Guroff et al., 1977). The reaction was stopped by addition of 1 μl 0.5 M EDTA, and incorporated radioactivity was determined as described previously (Tamura and Takano, 1978).

VSV based-pseudotyped viruses

Recombinant VSV, VSVΔG*/GFP-G, was kindly provided by Dr. Whitt. The virus carries the jellyfish GFP gene in place of the viral G protein gene, and its G protein is supplemented by a separate expression vector (Takada et al., 1997). The *env* genes of F-, A8, and PVC-211 MLVs were each cloned into a pCAGGS expression vector (pCAGGS-F-env, pCAGGS-A8-env, and pCAGGS-PVC-211-env, respectively). pCAGGS was kindly provided by Dr. Miyazaki, and transfected into 293T cells. To prepare VSV-based pseudotyped viruses, the cells were infected 24 h after transfection with VSVΔG*/GFP-G at an MOI of 10. After 12 h, the supernatant of each culture was replaced with fresh medium, and the cells were cultured for an additional 12 h. The culture supernatants were then collected, passed through a 0.22 μm pore size filter and stored at −80 °C as VSV-based pseudotyped viruses: VSV/F-Env, VSV/A8-Env, and VSV/PVC-211-Env, carrying Env of F-, A8, and PVC-211 MLVs, respectively. 293T cells that had not been transfected with the Env expression vector were also infected with VSVΔG*/GFP-G for preparing VSV viruses-like particles lacking Env (VSV/ΔEnv). To measure viral titer, NIH 3T3 cells were infected with each of the pseudotyped viruses in the presence of 10 μg/ml of polybrene and, at 16 h post-infection, GFP-positive cells were counted by flow cytometry.

FACS analysis

Cells were harvested and washed twice with FACS buffer (phosphate-buffered saline [PBS] containing 0.25% FCS, 0.25% horse serum, and 0.1% sodium azide). Then, the cells were suspended in FACS buffer and analyzed for GFP expression using a FACSAria Cell Sorter (BD Biosciences).

Immunoblot analysis

Western blot analysis was performed on 293T cells transfected with pCAGGS-F-env, pCAGGS-A8-env, or pCAGGS-PVC-211-env vectors, or with virions of VSV/F-Env, VSV/A8-Env, VSV/PVC-211-Env, VSV/ΔEnv; Mock transfected cells were used as a control. Cells were harvested at 48 h after transfection with the *env* expression vector. Cells were washed with PBS and then lysed with 2% sodium dodecyl sulfate (SDS) and 0.5 mM phenylmethylsulfonyl fluoride (PMSF) in PBS at 100 °C for 5 min. Nucleic acid was mechanically sheared using a syringe with a 22-gauge needle. A 1 ml aliquot of each virus supernatant, containing the 2×10^5 infectious units, was then subjected to ultracentrifugation at 30,000 rpm in a Beckman SW 41 Ti

rotor at 4 °C for 2 h to purify the virions. Precipitates containing virions were suspended in PBS. Sample buffer (5×) containing SDS, DTT, glycerol, and bromophenol blue in Tris–HCl (pH 6.8) was added to the cell lysate or the virion suspension. After boiling for 5 min, the lysates were loaded on a 10% SDS-polyacrylamide gel and electrophoresed. The proteins were then transferred to an Immobilon P membrane (Millipore) by electroblotting. To detect the Env protein, goat anti-Rauscher MLV gp70 (Quality Biotech Incorporated-Resource Laboratory) was used. Actin was detected using rabbit anti-beta-actin (Santa Cruz Biotechnology) as a loading control. Horseradish peroxidase-conjugated anti-goat IgG antibody and horseradish peroxidase-conjugated anti-rabbit IgG antibody (Santa Cruz Biotechnology) were used as secondary antibodies. The membrane was developed with ECL plus reagents (GE Healthcare). Band images were captured with LAS-3000 (FUJIFILM).

Preparation of VSV based-pseudotyped viruses for SPR analysis

Suspensions of VSV/F-Env, VSV/A8-Env, or VSV/PVC-211-Env (1×10^6 infectious units) were made up to 5 ml by adding fresh culture medium; they were then dialyzed in a cellulose tube (EIDIA Co., Ltd.) against 200× PBS (v/v) for 24 h at 4 °C, with the outer solution refreshed four times. Then, the solutions were fixed with 2% paraformaldehyde (PFA) buffered with 0.12 M phosphate (pH7.3). To remove the PFA, the solutions were dialyzed in a cellulose tube against 200× PBS (v/v) for 24 h at 4 °C, with the outer solution refreshed four times. Then, the solutions were concentrated at 4 °C to 0.5 ml (2×10^6 infectious units/ml) using an Amicon Ultra-15 100 K Centrifugal Filter Device (Millipore) and stored at −80 °C until use. For the negative control, we used an aliquot of the culture supernatant of VSV/ΔEnv-producing 293T cells; for the Mock control, we used an aliquot of the culture supernatant of 293T cells. For both controls, the aliquot was equivalent in volume to the sample from the culture supernatant of VSV/Env-producing cells, which contained 1×10^6 infectious units, and was treated in the same manner as above.

SPR analysis

Heparin, NAdOS-H and dNS-H were dialyzed against distilled water using an MWCO3500 membrane (SpectroPore), lyophilized, and then conjugated with an f-mono linker molecule to prepare the ligand conjugate as previously described (Sato et al., 2009; Suda et al., 2006). To prepare the Sugar Chip with immobilized ligand, the surface of a gold-coated chip (SUDx-Biotec) was oxidatively washed with UV ozone cleaner (Structure Probe Inc.) for 20 min and then immersed in 1 μM of the ligand conjugate dissolved in 50% (v/v) methanol solution overnight at room temperature with gentle agitation. The Sugar Chip was washed sequentially with water, 0.05% Tween 20, and water and dried at room temperature. For the SPR analysis, the Sugar Chip was set on a prism with refraction oil (nD = 1.518, Cargill Laboratories Inc.) in an SPR apparatus (SPR670M, Moritex). The SPR measurements were performed at room temperature according to the manufacturer's instructions, using PBS containing 0.05% Tween 20 as the running buffer at a flow rate of 15 μl/min.

Acknowledgments

We thank Dr. M. A. Whitt for providing VSVΔG*/GFP-G, and Dr. J. Miyazaki for providing pCAGGS. This work was supported in part by funding from MEXT (Ministry of Education, Culture, Sports, Science and Technology), the Matching Fund for Private Universities, S0901015, 2009–2014.

References

Albritton, L.M., Tseng, L., Scadden, D., Cunningham, J.M., 1989. A putative murine ecotropic retrovirus receptor gene encodes a multiple membrane-spanning protein and confers susceptibility to virus infection. Cell 57, 659–666.

Batra, R.K., Olsen, J.C., Hoganson, D.K., Caterson, B., Boucher, R.C., 1997. Retroviral gene transfer is inhibited by chondroitin sulfate proteoglycans/glycosaminoglycans in malignant pleural effusions. J. Biol. Chem. 272, 11736–11743.

Capila, I., Linhardt, R.J., 2002. Heparin–protein interactions. Angew. Chem. 41, 391–412.

Cardin, A.D., Weintraub, H.J., 1989. Molecular modeling of protein–glycosaminoglycan interactions. Arteriosclerosis 9, 21–32.

Copeland, R., Balasubramaniam, A., Tiwari, V., Zhang, F., Bridges, A., Linhardt, R.J., Shukla, D., Liu, J., 2008. Using a 3-*O*-sulfated heparin octasaccharide to inhibit the entry of herpes simplex virus type 1. Biochemistry 47, 5774–5783.

Crublet, E., Andrieu, J.P., Vives, R.R., Lortat-Jacob, H., 2008. The HIV-1 envelope glycoprotein gp120 features four heparan sulfate binding domains, including the co-receptor binding site. J. Biol. Chem. 283, 15193–15200.

Czub, M., Czub, S., McAtee, F.J., Portis, J.L., 1991. Age-dependent resistance to murine retrovirus-induced spongiform neurodegeneration results from central nervous system-specific restriction of virus replication. J. Virol. 65, 2539–2544.

Davis, H.E., Morgan, J.R., Yarmush, M.L., 2002. Polybrene increases retrovirus gene transfer efficiency by enhancing receptor-independent virus adsorption on target cell membranes. Biophys. Chem. 97, 159–172.

Davis, H.E., Rosinski, M., Morgan, J.R., Yarmush, M.L., 2004. Charged polymers modulate retrovirus transduction via membrane charge neutralization and virus aggregation. Biophys. J. 86, 1234–1242.

Fass, D., Davey, R.A., Hamson, C.A., Kim, P.S., Cunningham, J.M., Berger, J.M., 1997. Structure of a murine leukemia virus receptor-binding glycoprotein at 2.0 angstrom resolution. Science 277, 1662–1666.

Guibinga, G.H., Miyanohara, A., Esko, J.D., Friedmann, T., 2002. Cell surface heparan sulfate is a receptor for attachment of envelope protein-free retrovirus-like particles and VSV-G pseudotyped MLV-derived retrovirus vectors to target cells. Mol. Ther. 5, 538–546.

Hallak, L.K., Spillmann, D., Collins, P.L., Peeples, M.E., 2000. Glycosaminoglycan sulfation requirements for respiratory syncytial virus infection. J. Virol. 74, 10508–10513.

Jinno-Oue, A., Oue, M., Ruscetti, S.K., 2001. A unique heparin-binding domain in the envelope protein of the neuropathogenic PVC-211 murine leukemia virus may contribute to its brain capillary endothelial cell tropism. J. Virol. 75, 12439–12445.

Kai, K., Furuta, T., 1984. Isolation of paralysis-inducing murine leukemia viruses from Friend virus passaged in rats. J. Virol. 50, 970–973.

Kim, J.W., Closs, E.I., Albritton, L.M., Cunningham, J.M., 1991. Transport of cationic amino acids by the mouse ecotropic retrovirus receptor. Nature 352, 725–728.

Krusat, T., Streckert, H.J., 1997. Heparin-dependent attachment of respiratory syncytial virus (RSV) to host cells. Arch. Virol. 142, 1247–1254.

Landazuri, N., Le Doux, J.M., 2004. Complexation of retroviruses with charged polymers enhances gene transfer by increasing the rate that viruses are delivered to cells. J. Gene Med. 6, 1304–1319.

Le Doux, J.M., Morgan, J.R., Snow, R.G., Yarmush, M.L., 1996. Proteoglycans secreted by packaging cell lines inhibit retrovirus infection. J. Virol. 70, 6468–6473.

Le Doux, J.M., Morgan, J.R., Yarmush, M.L., 1999. Differential inhibition of retrovirus transduction by proteoglycans and free glycosaminoglycans. Biotechnol. Prog. 15, 397–406.

Masuda, M., Remington, M.P., Hoffman, P.M., Ruscetti, S.K., 1992. Molecular characterization of a neuropathogenic and nonerythroleukemogenic variant of Friend murine leukemia virus PVC-211. J. Virol. 66, 2798–2806.

Masuda, M., Hanson, C.A., Dugger, N.V., Robbins, D.S., Wilt, S.G., Ruscetti, S.K., Hoffman, P.M., 1997. Capillary endothelial cell tropism of PVC-211 murine leukemia virus and its application for gene transduction. J. Virol. 71, 6168–6173.

Mondor, I., Ugolini, S., Sattentau, Q.J., 1998. Human immunodeficiency virus type 1 attachment to HeLa CD4 cells is CD4 independent and gp120 dependent and requires cell surface heparans. J. Virol. 72, 3623–3634.

Neyts, J., Snoeck, R., Schols, D., Balzarini, J., Esko, J.D., Van Schepdael, A., De Clercq, E., 1992. Sulfated polymers inhibit the interaction of human cytomegalovirus with cell surface heparan sulfate. Virology 189, 48–58.

Oliff, A.I., Hager, G.L., Chang, E.H., Scolnick, E.M., Chan, H.W., Lowy, D.R., 1980. Transfection of molecularly cloned Friend murine leukemia virus DNA yields a highly leukemogenic helper-independent type C virus. J. Virol. 33, 475–486.

Patel, M., Yanagishita, M., Roderiquez, G., Bou-Habib, D.C., Oravecz, T., Hascall, V.C., Norcross, M.A., 1993. Cell-surface heparan sulfate proteoglycan mediates HIV-1 infection of T-cell lines. AIDS Res. Hum. Retroviruses 9, 167–174.

Pizzato, M., Marlow, S.A., Blair, E.D., Takeuchi, Y., 1999. Initial binding of murine leukemia virus particles to cells does not require specific Env-receptor interaction. J. Virol. 73, 8599–8611.

Rider, C.C., Coombe, D.R., Harrop, H.A., Hounsell, E.F., Bauer, C., Feeney, J., Mulloy, B., Mahmood, N., Hay, A., Parish, C.R., 1994. Anti-HIV-1 activity of chemically modified heparins: correlation between binding to the V3 loop of gp120 and inhibition of cellular HIV-1 infection in vitro. Biochemistry 33, 6974–6980.

Robert-Guroff, M., Schrecker, A.W., Brinkman, B.J., Gallo, R.C., 1977. DNA polymerase gamma of human lymphoblasts. Biochemistry 16, 2866–2873.

Sato, M., Ito, Y., Arima, N., Baba, M., Sobel, M., Wakao, M., Suda, Y., 2009. High-sensitivity analysis of naturally occurring sugar chains, using a novel fluorescent linker molecule. J. Biochem. 146, 33–41.

Secchiero, P., Sun, D., De Vico, A.L., Crowley, R.W., Reitz Jr., M.S., Zauli, G., Lusso, P., Gallo, R.C., 1997. Role of the extracellular domain of human herpesvirus 7 glycoprotein B in virus binding to cell surface heparan sulfate proteoglycans. J. Virol. 71, 4571–4580.

Shukla, D., Liu, J., Blaiklock, P., Shworak, N.W., Bai, X., Esko, J.D., Cohen, G.H., Eisenberg, R.J., Rosenberg, R.D., Spear, P.G., 1999. A novel role for 3-O-sulfated heparan sulfate in herpes simplex virus 1 entry. Cell 99, 13–22.

Suda, Y., Arano, A., Fukui, Y., Koshida, S., Wakao, M., Nishimura, T., Kusumoto, S., Sobel, M., 2006. Immobilization and clustering of structurally defined oligosaccharides for sugar chips: an improved method for surface plasmon resonance analysis of protein–carbohydrate interactions. Bioconjug. Chem. 17, 1125–1135.

Takada, A., Robison, C., Goto, H., Sanchez, A., Murti, K.G., Whitt, M.A., Kawaoka, Y., 1997. A system for functional analysis of Ebola virus glycoprotein. Proc. Natl. Acad. Sci. U. S. A. 94, 14764–14769.

Takase-Yoden, S., Watanabe, R., 1997. Unique sequence and lesional tropism of a new variant of neuropathogenic Friend murine leukemia virus. Virology 233, 411–422.

Tamura, T.-A., Takano, T., 1978. A new, rapid procedure for the concentration of C-type viruses from large quantities of culture media: ultrafiltration by diaflo membrane and purification by ficoll gradient centrifugation. J. Gen. Virol. 41, 135–141.

Trybala, E., Bergström, T., Spillmann, D., Svennerholm, B., Olofsson, S., Flynn, S.J., Ryan, P., 1996. Mode of interaction between pseudorabies virus and heparan sulfate/heparin. Virology 218, 35–42.

Trybala, E., Liljeqvist, J.A., Svennerholm, B., Bergström, T., 2000. Herpes simplex virus types 1 and 2 differ in their interaction with heparan sulfate. J. Virol. 74, 9106–9114.

Walker, S.J., Pizzato, M., Takeuchi, Y., Devereux, S., 2002. Heparin binds to murine leukemia virus and inhibits Env-independent attachment and infection. J. Virol. 76, 6909–6918.

Wang, H., Kavanaugh, M.P., North, R.A., Kabat, D., 1991. Cell-surface receptor for ecotropic murine retroviruses is a basic amino-acid transporter. Nature 352, 729–731.

Watanabe, R., Takase-Yoden, S., 1995. Gene expression of neurotropic retrovirus in the CNS. Prog. Brain Res. 105, 255–262.

WuDunn, D., Spear, P.G., 1989. Initial interaction of herpes simplex virus with cells is binding to heparan sulfate. J. Virol. 63, 52–58.

Xia, G., Chen, J., Tiwari, V., Ju, W., Li, J.P., Malmstrom, A., Shukla, D., Liu, J., 2002. Heparan sulfate 3-O-sulfotransferase isoform 5 generates both an antithrombin-binding site and an entry receptor for herpes simplex virus, type 1. J. Biol. Chem. 277, 37912–37919.

Ye, S., Luo, Y., Lu, W., Jones, R.B., Linhardt, R.J., Capila, I., Toida, T., Kan, M., Pelletier, H., McKeehan, W.L., 2001. Structural basis for interaction of FGF-1, FGF-2, and FGF-7 with different heparan sulfate motifs. Biochemistry 40, 14429–14439.

DOI: 10.1002/chem.201003357

The First Total Synthesis of Ganglioside GalNAc-GD1a, a Target Molecule for Autoantibodies in Guillain–Barré Syndrome**

Kohki Fujikawa,[a, b] Shinya Nakashima,[a, b] Miku Konishi,[a] Tomoaki Fuse,[a] Naoko Komura,[a, b] Takayuki Ando,[a, b] Hiromune Ando,*[a, b] Nobuhiro Yuki,[c] Hideharu Ishida,*[a] and Makoto Kiso[a, b]

Abstract: The first synthesis of ganglioside GalNAc-GD1a, featuring efficient glycan assembly and a cyclic glucosyl ceramide as a versatile unit for ganglioside synthesis is described. Although ganglioside GalNAc-GD1a was first found as a brain ganglioside, IgG autoantibodies to GalNAc-GD1a were subsequently found to be closely related to a human peripheral-nerve disorder, Guillain–Barré syndrome, which is the commonest cause of acute flaccid paralysis worldwide. In this study, the characteristic hexasaccharide part carrying two sialic acid residues was synthesized efficiently by use of a readily accessible GM2-core unit as a common unit. The potentially difficult coupling of the oligosaccharide and ceramide moieties was carried out by using a cyclic glucosyl ceramide as a coupling partner for the hexasaccharide part, thereby successfully providing the framework of the target compound. Global deprotection delivered the homogenous ganglioside GalNAc-GD1a. An enzyme-linked immunosorbent assay showed that sera from patients with Guillain–Barré syndrome reacted both with natural and with synthetic GalNAc-GD1a.

Keywords: gangliosides · Guillain–Barré syndrome · natural products · sialic acids · total synthesis

Introduction

Gangliosides are a family of sialic acid containing glycosphingolipids that are highly concentrated in nervous tissues. Autoantibodies to gangliosides are useful diagnostic markers in autoimmune neuropathies, at least some of which are involved in pathogenesis.[1] The ceramide portion of the ganglioside is anchored in the lipid bilayer membrane with the carbohydrate structure exposed outside the cell, where it acts as an autoantibody target. Guillain–Barré syndrome (GBS) is now the most frequent cause of acute flaccid paralysis worldwide because the incidence of poliomyelitis has been much reduced by immunization. GBS is mainly divided into two subtypes: acute inflammatory demyelinating polyneuropathy and acute motor axonal neuropathy.[2] IgG autoantibodies against gangliosides GM1, GM1b, GD1a, and GalNAc-GD1a are strongly associated with the latter subtype. In other words, IgG anti-GM1, -GM1b, -GD1a, and -GalNAc-GD1a antibodies are diagnostic markers of GBS. Currently, anti-GM1 and -GD1a antibodies are measured at some commercial laboratories, and the measurement kits are also available for investigators. The antigens GM1 and GD1a are abundant and are easily purified from bovine brain gangliosides. GM1b and GalNAc-GD1a are not as readily available, being difficult to isolate from mixtures of bovine brain gangliosides. Few researchers are able to test the autoantibodies against GM1b or GalNAc-GD1a antigens. However, there are some GBS patients who have only anti-GM1b and -GalNAc-GD1a antibodies, and not anti-GM1 or -GD1a antibodies.[3] The aim of this study was to provide a method of synthesizing large quantities of GalNAc-GD1a.[4] Very recently, we briefly reported the assembly of GalNAc-GD1a as an example of the application of a new synthetic method for the synthesis of gangliosides.[5] Here we present a detailed report of the first total synthesis of GalNAc-GD1a.

[a] Dr. K. Fujikawa, S. Nakashima, M. Konishi, T. Fuse, N. Komura, Dr. T. Ando, Dr. H. Ando, Dr. H. Ishida, Dr. M. Kiso
Department of Applied Bioorganic Chemistry
Gifu University
1-1 Yanagido, Gifu-shi, Gifu 501-1193 (Japan)
Fax: (+81) 58-293-3452, (+81) 58-293-2918
hando@ gifu-u.ac.jp,
E-mail: ishida@gifu-u.ac.jp

[b] Dr. K. Fujikawa, S. Nakashima, N. Komura, Dr. T. Ando, Dr. H. Ando, Dr. M. Kiso
Department of Applied Bioorganic Chemistry
Institute for Integrated Cell-Material Sciences (WPI program)
Kyoto University
Yoshida Ushinomiya-cho, Sakyo-ku, Kyoto 606-8501 (Japan)

[c] Dr. N. Yuki
Departments of Microbiology & Medicine
National University of Singapore
5 Science Drive 2, Blk MD4A, Level 5
Singapore 117597 (Singapore)

[**] Part 153 of the series: Synthetic studies on sialoglycoconjugates; for Part 152, see: H. Tamai, H. Ando, H.-N. Tanaka, H. Ishida, M. Kiso, *Angew. Chem.* **2011**, *10*, 2378–2381; *Angew. Chem. Int. Ed.* **2011**, *10*, 2330–2333.

Supporting information for this article is available on the WWW under http://dx.doi.org/10.1002/chem201003357.

Results and Discussion

The structure and retrosynthetic analysis of the target compound **1** is illustrated in Scheme 1. The target molecule was disassembled at the β(1,4)-linkage between galactose (Gal) and glucose (Glc) by an approach based on the use of the glucosyl–ceramide (Glc–Cer) cassette **3**, which was developed by our research group,[5,6] thus providing **3** and the hexasaccharide fragment **2**. The approach based on use of the Glc–Cer cassette is useful in that it avoids loss of the valuable oligosaccharide unit in a coupling reaction with the lipophilic, self-aggregating, bulky, and unreactive ceramide moiety. The physical properties of Cer were much improved by combining Glc with Cer. It was also demonstrated that the steric bulk of the Cer moiety did not reduce the reactivity of the C4 hydroxy group in glycosylation with the oligosaccharyl donor. However, in view of the overall efficiency of the chemical synthesis, the low yield of the coupling between Glc and Cer needed to be improved. This issue was very recently overcome by the development of an intramolecular glycosylation system, and the resulting cyclic Glc–Cer acceptor was shown to be capable of accepting a variety of oligosaccharide donors.[5] In this study, we attempted to elaborate the design and synthetic process of the cyclic Glc–Cer acceptor **3** further from the perspective of overall efficiency.

To access the hexasaccharide moiety **2**, that is, the tandem sequence of the GM2-core trisaccharide, we designed a convergent approach in which the GM2-core trisaccharide **4** could serve as a pivotal common unit. We envisaged a one-step conversion of **4** into the corresponding glycosyl acceptor through the 3-*O* to 2-*N* migration of the acetyl group upon deprotection of the C2 amine group. The unit **4** was further disconnected into the 3-*O*-acetyl galactosaminyl donor **5** and the sialyl galactose unit **6**.

To achieve migration of the acetyl group from O to N, we chose a selectively removable 2,2,2-trichloroethoxycarbonyl (Troc) group for the protection of the C2 amine group and as a stereodirecting element during the glycosylation reaction. The C4 and C6 hydroxy groups would be protected by acetate, leading to the triacetate galactosamine (GalN) derivative **7**, which could easily be produced from galactosamine (Scheme 2).[7] The structure of the coupling partner for the GalN donor **7** was designed according to a previously reported GM2-core trisaccharide synthesis.[7a] The *N*-Troc sialyl galactoside **8**,[8] which can be produced on a large scale because it can be purified by crystallization, was converted in high yield into the corresponding *N*-acetyl compound **9** by treatment with zinc in acetic anhydride.[9] The C4 free hydroxy group of **9** was then glycosylated with the GalN donor **7**, by use of *N*-iodosuccinimide (NIS)/trifluoromethanesulfonic acid (TfOH)[10] in CH_2Cl_2 at 0 °C, to pro-

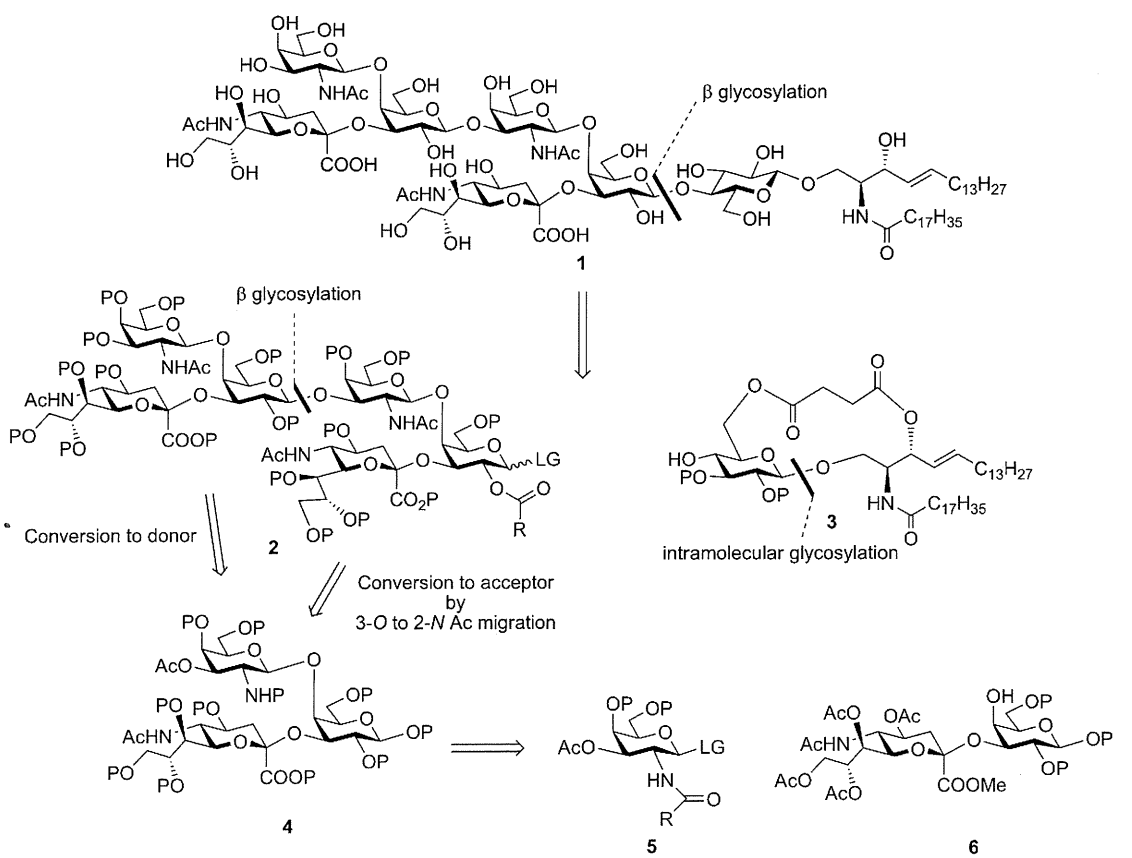

Scheme 1. Retrosynthetic analysis of the target compound **1**. P = protecting group, LG = leaving group.

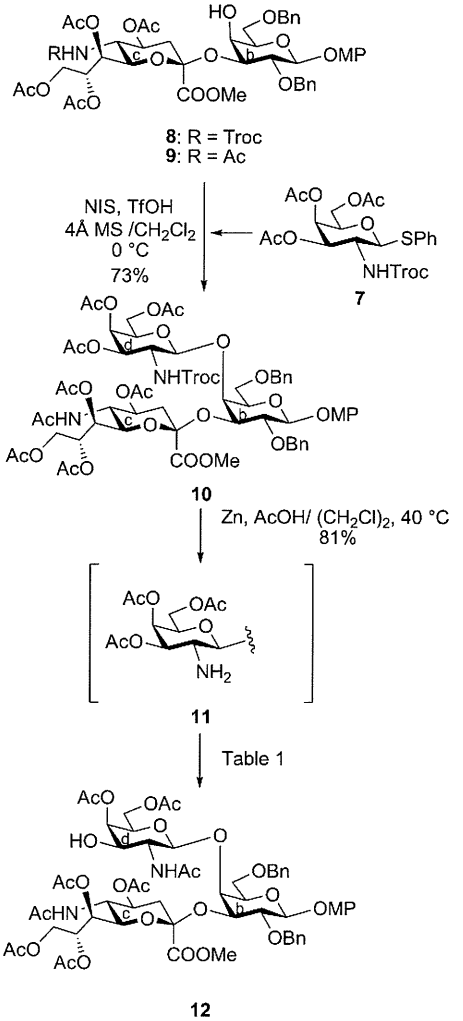

Scheme 2. Synthesis of the GM2-core acceptor **12**. Bn = benzyl, Troc = 2,2,2-trichloroethoxycarbonyl, MP = *p*-methoxyphenyl, NIS = *N*-iodosuccinimide, TfOH = trifluoromethanesulfonic acid, MS = molecular sieves.

duce the GM2-core structure **10**. The core structure was divided into separate portions, which were then converted into the corresponding glycosyl donor and acceptor.

To achieve rapid liberation of the GalN C3 hydroxy group by migration of the acetyl group from O to N, we first removed the Troc protection with zinc in acetic acid to obtain the amino GM2-core unit **11** in 81% yield. The acetyl migration was next investigated and the results are summarized in Table 1. Under basic conditions, the migration of the acetyl group at the C3 position was very sluggish, providing poor to marginal yields (Table 1, entries 1 and 2). In addition, the methyl ester moiety of the sialic acid was hydrolyzed to afford a carboxylic acid derivative (Table 1, entry 1). In contrast, acidic conditions provided a much better yield (74%), which demonstrated the validity of our strategy. In the next step, we attempted a conversion of **10** into **12** in a one-pot reaction. As a result, the *N*-Troc-protected compound **10** could be converted into **12** in 70% yield by treatment with zinc in AcOH/DMF (1:9) at 60 °C (Table 1, entry 4).

Table 1. Examination of 3-*O* to 2-*N* acetyl migration to produce the GM2-core acceptor **12**.

Entry	Reagent/solvent	*T* [°C]	*t* [h]	Yield [%]
1	TEA/DMF 1:1	60	48	trace
2	Pyr/DCE 1:1	60	24	58
3	AcOH/1,4-dioxane 1:4	60	48	74
4[a]	Zn, AcOH/DMF (1:9)	60	15	70

[a] One-pot reaction from compound **10**. TEA = triethylamine, Pyr = pyridine, DCE = 1,2-dichloroethane.

On the other hand, the trisaccharide **10** was also transformed into the corresponding trichloroacetimidate donor **13** through a six-step reaction sequence by a previously reported procedure[7a] (58% overall yield) as shown in Scheme 3.

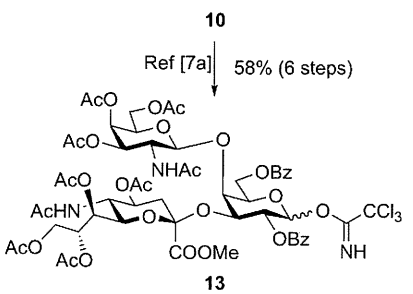

Scheme 3. Synthesis of the GM2-core donor **13**. a) i) Zn, AcOH/MeOH (1:1), RT; ii) Ac_2O/Pyr, RT, 81%; b) i) H_2, $Pd(OH)_2$-C/1,4-dioxane, RT; ii) Bz_2O, DMAP/Pyr, RT, 95%; c) i) CAN, MeCN/PhMe/H_2O (6:5:3), RT; ii) CCl_3CN, DBU/CH_2Cl_2, RT, 75%. Bz = benzoyl, CAN = ceriu-m(IV) ammonium nitrate.

To assemble the tandem sequence of the GM2-core trisaccharides, the trisaccharyl donor **13** (1.0 equiv) and the acceptor **12** (1.0 equiv) were coupled in CH_2Cl_2 at 0 °C in the presence of a catalytic amount of TMSOTf (0.16 equiv), yielding the highly branched disialoside **14** as a single β-isomer in 70% yield (Scheme 4). This encouraging result suggests that compound **12** could be usable as a common acceptor for the construction of other core sequences of a series of gangliosides such as GM1, GD1a, and GT1a. For comparison, the coupling yield of **12** and **13** is much higher than those of similar glycosylations performed in our research group: the coupling of the 6-*O*-acetyl-4-*O*-benzyl GM2 acceptor **18** with the small sialyl galactosyl imidate donor **19**, for example, afforded a lower yield (38%) of **20**, even when two equivalents of the donor were used (Scheme 5).[11] This suggests that coupling through the C3 hydroxy group is disfavored by the presence of a bulky substituent, rather than an electron-withdrawing one, at the C4 position. The hexasaccharide **14** (Scheme 4) was then converted into the imidate donor **17** in three steps: replacement of the benzyl groups with benzoyl groups (i) H_2, $Pd(OH)_2$-C; ii) Bz_2O, DMAP, Pyr, 92%), removal of the *p*-methoxyphenyl group (CAN, H_2O, 70%), and conversion of the resulting

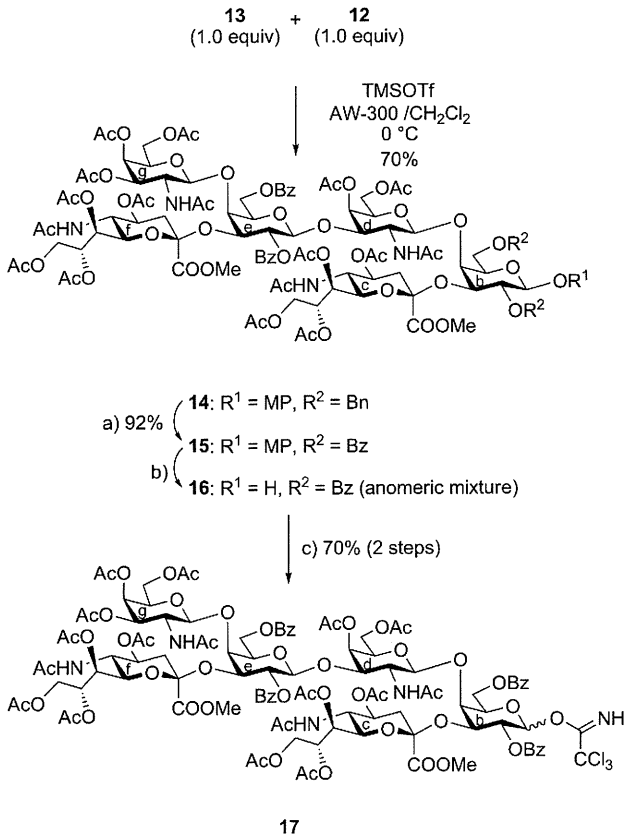

Scheme 4. Assembly of the GM2-core tandem sequence and conversion into the corresponding glycosyl donor **17**. a) i) H_2, $Pd(OH)_2$-C/1,4-dioxane, RT; ii) Bz_2O, DMAP/Pyr, RT, 92%; b) CAN, MeCN/PhMe/H_2O (6:5:3), RT, 70%; c) CCl_3CN, DBU/CH_2Cl_2, RT, 70% (2 steps). TMSOTf = trimethylsilyl trifluoromethanesulfonate, DMAP = 4-dimethylaminopyridine, DBU = 1,8-diazabicyclo[5.4.0]undec-7-ene.

hydroxy group into a trichloroacetimidate group (quantitative),[12] to give the hexasaccharyl donor **17** in high yields.

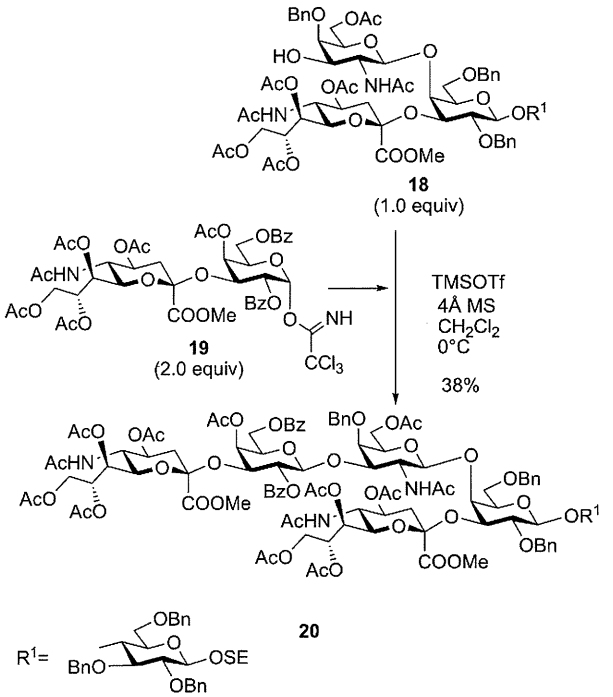

Scheme 5. Previously obtained result for the glycosylation of the GM2 tetrasaccharide acceptor **18** with the sialyl galactosyl donor **19**. SE = 2-(trimethylsilyl)ethyl.

The cyclic Glc–Cer acceptor **25** was synthesized as the first coupling partner for the hexasaccharide **17** (Scheme 6). This synthesis began with tethering of the Glc donor and Cer through a succinoyl bridge.[13] The succinoylated Cer derivative **21**[14] and the 4,6-diol thioglucoside **22**[15] could thus be condensed with the aid of a carbodiimide coupling reagent (EDC·HCl) and a catalytic amount of DMAP to give the tethered compound **23**. The free hydroxy group at the C1 position of the Cer moiety was retrieved by exposure to TBAF. Then, intramolecular coupling within **24**, promoted

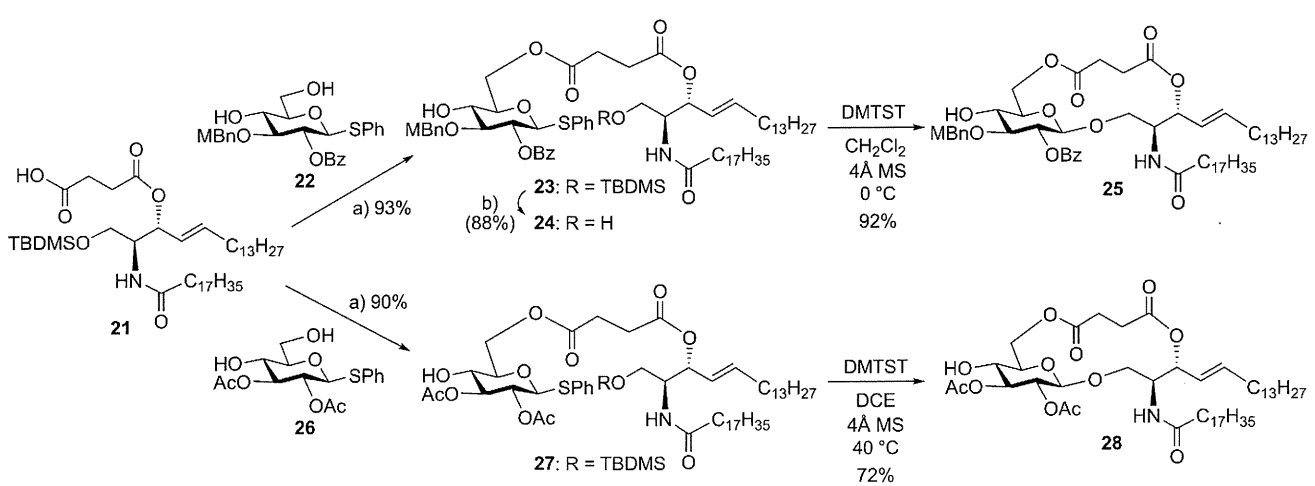

Scheme 6. Synthesis of the cyclic Glc–Cer acceptors **25** and **28** through intramolecular glycosylation. a) EDC·HCl, DMAP/CH_2Cl_2, RT, 93%; b) TBAF, AcOH/THF, 0 °C to RT, 88%. TBDMS = *tert*-butyldimethylsilyl, MBn = *p*-methoxybenzyl, EDC = 1-ethyl-3-(3-dimethylaminopropyl)carbodiimide, TBAF = *n*-tetrabutylammonium fluoride, DMTST = dimethyl(methylthio)sulfonium trifluoromethanesulfonate, DCE = 1,2-dichloroethane.

by DMTST,[16] successfully produced the cyclic Glc–Cer acceptor **25** in very high yield without affecting the C4–C5 olefin moiety (use of NIS/TfOH as the promoter did not leave the olefin intact).

In the next step, the 2,3-diacetyl Glc–Cer **28** was designed as a more easily accessible version of the cyclic Glc–Cer **25**. The 2,3-diacetyl thioglucoside **26**[17] was tethered to the Cer unit **21** in a similar way to compound **23**, producing **27** in high yield. To reduce the number of reaction steps, compound **27**, with the TBDMS-protected C1 hydroxy group, was subjected to direct DMTST-promoted intramolecular glycosylation. At room temperature, this reaction was complete after 3 h and gave the cyclic Glc–Cer **28** in 36% yield. In contrast, at 40 °C the reaction gave a yield of 72%. During this reaction, the acetyl group at C3 did not migrate to the adjacent C4 hydroxy group; to the best of our knowledge this is the first example of intramolecular glycosylation of a TBDMS-protected hydroxy group.[18] It is unlikely that compound **23**, with an acid-labile MBn group, would undergo such a direct glycosylation. The cyclic Glc–Cer **28** was synthesized more efficiently than **25** with respect to the overall yields based on glucose pentaacetate: the overall yield for **28** was 43% (seven steps), whereas that of **25** was 27% (nine steps).

The above cyclic Glc–Cer acceptors were next subjected to model glycosylation reactions with the GM2-core donor **13** to evaluate their potentials as glycosyl acceptors (Scheme 7). Equimolar amounts of the glycosyl donor **13** and the Glc–Cer acceptor (**25** or **28**) were allowed to react in the presence of a TMSOTf catalyst in $CHCl_3$ at 0 °C. This model experiment revealed distinct differences in reactivity between the two cyclic Glc–Cer acceptors. Compound **25** gave the glycosidated product in 70% yield, almost 1.5 times that achieved with **28** (48%). Furthermore, use of a linear analogue (**29**) of compound **28** reduced the coupling yield to 28%. It was observed that the presence of an electron-donating group was more suitable for protection of the C3 hydroxy group even if it was bulky. In addition, the results for cyclic versus linear acceptors indicated that the C4 hydroxy group in the cyclic structure was more reactive than that in the linear analogue. In the ^{1}H NMR spectrum for compound **28**, the coupling constants between H5 and H6 or H6′ were 9.7 and 2.3 Hz, respectively. These coupling constants were used to estimate the population of rotamers about the C5–C6 bond by a previously reported method based on Karplus relationships.[19] The estimation showed that the *gauche/trans* (*gt*) rotamer was predominant (83%) over the *gauche/gauche* (*gg*) (19%) and *trans/gauche* (*tg*) rotamers (−2%). The *gt* rotamer of **28** is illustrated in Scheme 8. In contrast, the *gg* rotamer was favored (71%) over the *gt* (26%) and *tg* (3%) rotamers about the C5–C6 bond in **29** ($J(5,6)=4.1$ Hz and $J(5,6')=2.0$ Hz), due to the *gauche* effect[20] between σ_{C5-H5} and σ^*_{C6-O6}. These results are consistent with those reported for the conformational analysis of the 6-*O*-acetyl glucose derivative.[19b] This comparison of conformations about the C5–C6 bonds of **28** and **29** suggests that the acetyl group at the C6 position reduced the reactivity of the C4 hydroxy group through steric hindrance rather than through its electron-withdrawing effect.

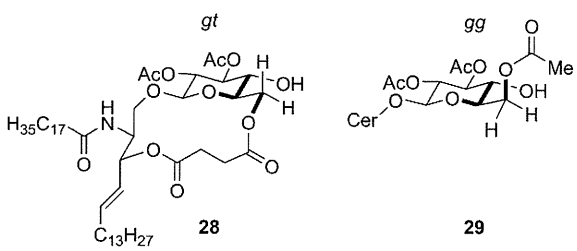

Scheme 8. Structures of predominant rotamers about C5–C6 bonds within compounds **28** and **29** based on estimation with the aid of Karplus relationships.

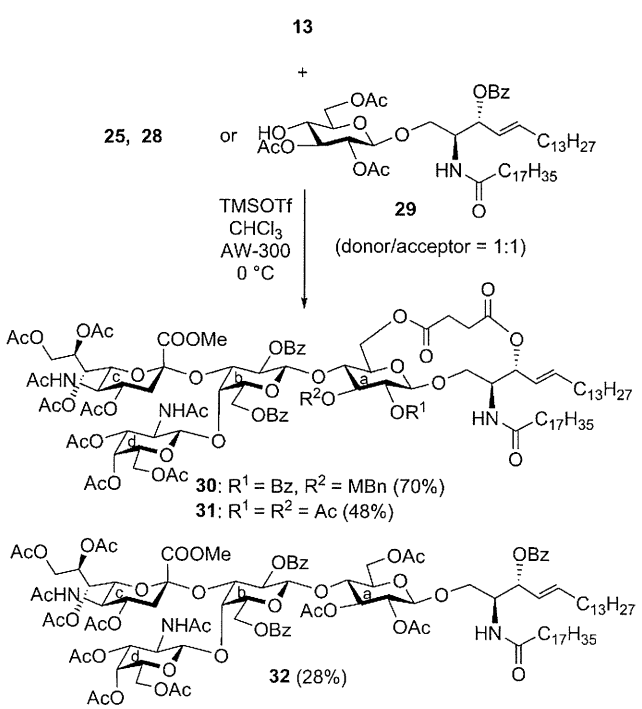

Scheme 7. Examination of the glycosylation of the Glc–Cer acceptors **25**, **28**, and **29**.

Although we could have used the easily accessible Glc–Cer acceptor **28**, as mentioned above, the Glc–Cer acceptor **25** was chosen as the coupling partner for the hexasaccharyl donor **17**, to take advantage of the high coupling yield. To our delight, the most challenging coupling reaction in this study, between **17** (1.0 equiv) and **25** (1.0 equiv) in the presence of catalytic TMSOTf in $CHCl_3$ at room temperature, successfully delivered the glycolipid framework **33** in 60% yield, as shown in Scheme 9. Next, compound **33** was converted into compound **34** (TFA, 0 °C). Compound **34** was then deacylated by the Zemplén method, and saponification of the methyl ester group gave the target compound **1**. The first attempt at this synthetic route produced 20 mg of ho-

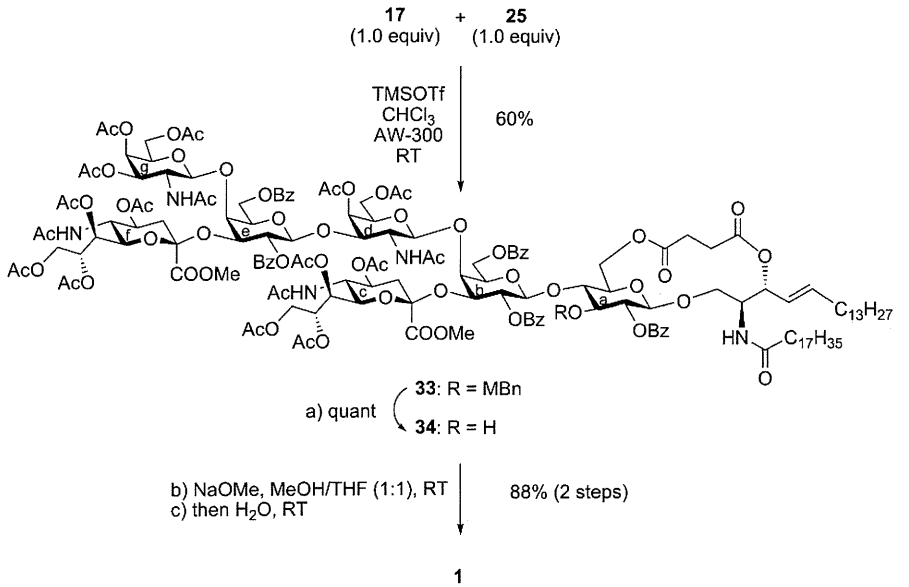

Scheme 9. Final approach to target compound **1**. a) TFA/CH_2Cl_2, 0 °C, quant. TFA = trifluoroacetic acid.

mogenous ganglioside GalNAc-GD1a **1**, which was then subjected to reaction with serum IgG antibodies from patients with GBS.

Natural GalNAc-GD1a was isolated from bovine brain gangliosides as previously reported.[3c] Sera were selected from 24 patients with GBS: twelve had high titers of IgG antibodies against the natural GalNAc-GD1a, whereas the remaining 12, who did not, acted as negative controls. IgG antibodies against the natural and synthetic GalNAc-GD1a (5 pmol per well) were measured in sera (1:500 dilution) from the patients by means of an enzyme-linked immunosorbent assay, as described previously.[3d] Figure 1 shows that the 12 sera with positive IgG antibodies against the natural GalNAc-GD1a bound to the synthetic GalNAc-GD1a, whereas none of the controls did. These results suggest that synthetic GalNAc-GD1a could be useful in autoantibody testing.

Conclusion

We have achieved the first total synthesis of ganglioside GalNAc-GD1a in sufficient quantities for biological study. The highly branched glycan structure comprising the tandem sequence of GM2-core trisaccharides was successfully constructed by an efficient route that used the highly accessible GM2-core unit **10** as a pivotal intermediate. The successful coupling of the huge hexasaccharyl donor **17** and the cyclic Glc–Cer **25** consequently led to delivery of the refined target molecule in sufficient quantities for biological study. With this total synthesis of the intricate ganglioside, the efficacy of the glucosyl ceramide cassette approach with the cyclic Glc–Cer was confirmed. Furthermore, the reactivity of the synthetic GalNAc-GD1a towards serum IgG from GBS patients was confirmed to be comparable to that of natural GalNAc-GD1a.

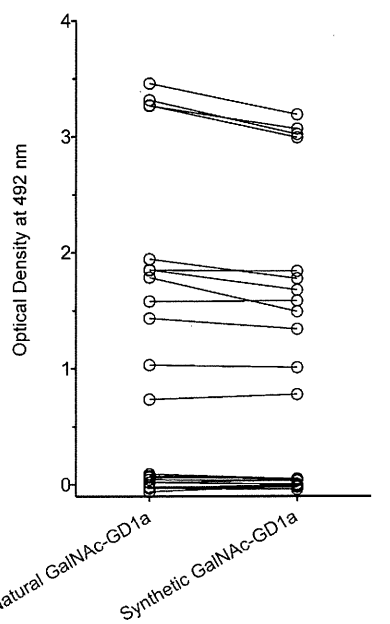

Figure 1. Enzyme-linked immunosorbent assay results in 24 patients with Guillain–Barré syndrome. Sera from 12 patients who had IgG antibodies to natural GalNAc-GD1a reacted with synthetic GalNAc-GD1a, whereas sera from 12 patients who had no IgG antibodies to the natural GalNAc-GD1a did not react with the synthetic GalNAc-GD1a.

Experimental Section

General procedures: ^1H and ^{13}C NMR spectra were recorded with JEOL JNM-ECA400, JNM-ECA500, and JNM-ECA600 spectrometers. ^1H NMR chemical shifts are expressed in ppm (δ) relative to the signal of Me_4Si as an internal standard. ^{13}C NMR chemical shifts are expressed in ppm (δ) relative to the signal of the solvent as a standard. High-resolution mass spectrometry (HRMS) was performed with a Bruker Daltonics micrOTOF (ESI-TOF) mass spectrometer. Specific rotations were measured with a Horiba SEPA-300 high-sensitivity polarimeter. Molecular sieves were purchased from Wako Chemicals and dried at 300 °C for 2 h in a muffle furnace prior to use. Reactions were carried out under argon unless otherwise specified. Solvents as reaction media were dried over molecular sieves and used without further purification. TLC analysis was performed with Merck TLC plates (silica gel $60F_{254}$ on glass). Compounds were visualized by exposure to UV light (254 nm) or by spraying either with H_2SO_4 solution in EtOH (10%) or with ninhydrin reagent, followed by heating. Flash column chromatography on silica gel (Fuji Silysia, 80 mesh and 300 mesh) was performed

with the solvent systems (v/v) specified. Evaporation and concentration were conducted in vacuo.

Compound 9: Zinc powder (1.0 g) was added at RT to a solution of **8** (1.00 g, 932 μmol) in a mixture of AcOH (10.0 mL), THF (10.0 mL), and Ac_2O (10.0 mL). The mixture was stirred for 3 h at RT (completion of the reaction was confirmed by TLC, $CHCl_3$/MeOH 18:1). The reaction mixture was filtered through Celite and the removed zinc powder was washed with EtOAc. The combined filtrate and washings were concentrated by co-evaporation with toluene. The residue was extracted with EtOAc and the organic layer was washed with saturated aqueous Na_2CO_3 and brine, dried (Na_2SO_4), and concentrated. The residue was purified by column chromatography on silica gel (EtOAc/hexane 5:2→3:1) to give **9** (786 mg, 90%). $[\alpha]_D=-14.9°$ ($c=0.9$, $CHCl_3$); ^1H NMR (600 MHz, $CDCl_3$): $\delta=7.42$–6.78 (m, 14H; 3×Ph), 5.42 (m, 1H; H-8c), 5.31 (dd, $J_{6,7}=2.1$ Hz, $J_{7,8}=8.3$ Hz, 1H; H-7c), 5.11 (d, $J_{5,NH}=9.6$ Hz, 1H; NH), 4.94 (d, $J_{1,2}=8.2$ Hz, 1H; H-1b), 4.92 (d, $J_{gem}=12.4$ Hz, 1H; PhCH_2), 4.87 (m, 1H; H-4c), 4.82 (d, 1H; PhCH_2), 4.60–4.55 (m, 2H; PhCH_2), 4.32 (dd, $J_{8,9}=2.4$ Hz, $J_{gem}=12.4$ Hz, 1H; H-9c), 4.26 (dd, $J_{2,3}=9.6$ Hz, $J_{3,4}=3.4$ Hz, 1H; H-3b), 4.09 (q, $J_{4,5}=J_{5,6}=9.6$ Hz, 1H; H-5c), 4.04 (dd, 1H; H-6c), 3.96 (dd, $J_{8,9'}=6.2$ Hz, 1H; H-9′c), 3.86–3.76 (m, 11H; H-2b, H-4b, H-5b, H-6b, H-6′b, OMe, COOMe), 2.77 (s, 1H; OH), 2.58 (dd, $J_{3eq,4}=4.2$ Hz, $J_{gem}=13.1$ Hz, 1H; H-3c$_{eq}$), 2.10–1.86 ppm (m, 16H; H-3c$_{ax}$, 5×Ac); ^{13}C NMR (150 MHz, $CDCl_3$): $\delta=170.8$, 170.5, 170.2, 170.1, 169.9, 168.5, 155.1, 151.6, 138.8, 138.1, 128.3, 128.1, 127.8, 127.6, 127.5, 127.4, 118.4, 114.4, 102.7, 97.9, 75.6, 74.9, 73.5, 73.0, 72.7, 69.3, 69.0, 68.8, 68.1, 67.3, 62.3, 55.6, 53.0, 49.1, 36.9, 23.1, 21.1, 20.7, 20.7, 20.6 ppm; HRMS: *m/z*: calcd for $C_{47}H_{57}NO_{19}Na^+$: 962.3417 $[M+Na]^+$; found: 962.3417.

Compound 10: Molecular sieves (4 Å, 10 g) were added to a solution of **7** (2.2 g, 3.94 mmol) and **9** (3.7 g, 3.94 mmol) in CH_2Cl_2 (80.0 mL). The suspension was stirred for 1 h at RT, after which NIS (2.3 g, 10.2 mmol) and TfOH (90 μL, 1.02 mmol) were added at 0 °C. Stirring was continued for 1 h at 0 °C (completion of the reaction was confirmed by TLC, EtOAc/hexane 3:1). The reaction mixture was filtered through Celite and the removed molecular sieves were washed with $CHCl_3$. The combined filtrate and washings were extracted with $CHCl_3$, and the organic layer was washed with saturated aqueous $NaHCO_3$, saturated aqueous $Na_2S_2O_3$, and brine, dried (Na_2SO_4), and concentrated. The residue was purified by column chromatography on silica gel (EtOAc/hexane 2:1) to give **10** (4.0 g, 73%). $[\alpha]_D=-16.0°$ ($c=1.0$, $CHCl_3$); ^1H NMR (600 MHz, $CDCl_3$): $\delta=7.28$ (m, 10H; 2×Ph), 7.07–6.81 (2×d, 4H; MeOA*r*), 6.20 (d, $J_{NH,2}=8.3$ Hz, 1H; NHd), 5.36 (m, 1H; H-4d), 5.23 (m, 4H; H-8c, H-7c, NHc, H-3d), 5.13 (m, 2H; H-4c, CH_2), 4.99 (d, $J_{1,2}=8.9$ Hz, 1H; H-1d), 4.95 (d, 1H; CH_2), 4.89 (d, $J_{1,2}=8.2$ Hz, 1H; H-1b), 4.57 (m, 3H; 2×CH_2), 4.33 (m, 2H; H-6d, CH_2), 4.21 (near t, $J_{6,6'}=11.0$ Hz, $J_{5,6'}=8.3$ Hz, 1H; H-6′d), 4.16 (m, 1H; H-2d), 4.09–3.97 (m, 6H; H-5d, H-4b, H-3b, H-9c, H-9′c, H-5c), 3.94 (s, 3H; OMe), 3.90 (dd, $J_{6,6'}=10.3$ Hz, $J_{6,5}=5.5$ Hz, 1H; H-6b), 3.78 (m, 6H; H-6c, H-6′b, H-2b, OMe), 3.67 (m, 1H; H-5b), 3.24 (m, 1H; H-3c$_{eq}$), 2.18–1.88 ppm (m, 25H; 8×Ac, H-3c$_{ax}$); ^{13}C NMR (150 MHz, $CDCl_3$): $\delta=170.6$, 170.4, 170.3, 170.3, 170.2, 169.6, 169.5, 168.5, 155.3, 154.5, 151.3, 138.2, 138.0, 128.3, 128.2, 127.8, 127.7, 127.6, 118.7, 118.5, 114.5, 102.9, 101.8, 99.2, 96.0, 78.6, 77.7, 75.6, 74.2, 73.6, 72.2, 71.9, 70.0, 69.4, 69.0, 67.5, 67.1, 66.6, 62.1, 61.2, 55.6, 53.5, 52.9, 49.0, 35.2, 23.1, 21.0, 20.7, 20.6, 20.5 ppm; HRMS: *m/z* calcd for $C_{62}H_{75}Cl_3N_2O_{28}Na^+$: 1423.3469 $[M+Na]^+$; found: 1423.3470.

Compound 12: Zinc powder (1.0 g) was added at RT to a solution of **10** (100 mg, 71 μmol) in a mixture of DMF (6.4 mL) and AcOH (0.7 mL). The mixture was stirred for 15 h at 60 °C (completion of the reaction was confirmed by TLC, EtOAc/MeOH 20:1). The reaction mixture was filtered through Celite and the removed zinc powder was washed with EtOAc. The combined filtrate and washings were extracted with EtOAc. The organic layer was washed with H_2O, saturated aqueous Na_2CO_3, and brine, dried (Na_2SO_4), and concentrated. The residue was purified by column chromatography on silica gel (EtOAc/MeOH 50:1) to give **12** (62 mg, 70%). $[\alpha]_D=-12.5°$ ($c=0.4$, $CHCl_3$); ^1H NMR (600 MHz, $CDCl_3$): $\delta=7.28$ (m, 10H; 2×Ph), 7.08–6.81 (m, 3H; NHd, MeOA*r*), 5.33 (d, $J_{3,OH}=3.4$ Hz, 1H; OH), 5.25 (m, 4H; H-8c, H-7c, H-4d, NHc), 5.08 (m, 2H; H-4c, PhCH_2), 4.92 (d, $J_{1,2}=7.6$ Hz, 1H; H-1b), 4.78 (d, $J_{1,2}=8.3$ Hz, 1H; H-1d), 4.56 (m, 3H; PhCH_2, PhCH_2), 4.18 (m, 2H; H-9c, H-3b), 4.11 (m, 2H; H-6d, H-4b), 4.05–3.96 (m, 5H; H-6′d, H-2d, H-3d, H-9′c, H-5c), 3.87 (m, 4H; OMe, H-6b), 3.78 (m, 7H; H-5d, H-6′b, H-2b, H-6c), 3.68 (m, 1H; H-5b), 2.30 (m, 2H; H-3c$_{eq}$, H-3c$_{ax}$), 2.16–1.91 ppm (8 s, 24H; 8×Ac); ^{13}C NMR (150 MHz, $CDCl_3$): $\delta=173.4$, 170.6, 170.5, 170.3, 169.6, 169.4, 168.0, 155.4, 151.1, 138.1, 137.7, 128.4, 128.3, 127.9, 127.8, 127.7, 127.6, 118.6, 114.5, 103.0, 101.5, 99.3, 78.5, 77.7, 77.3, 75.7, 75.5, 74.0, 73.8, 73.7, 72.4, 70.4, 69.5, 68.7, 68.6, 67.5, 66.7, 62.0, 61.9, 55.6, 55.3, 53.2, 49.0, 35.5, 29.7, 23.2, 22.6, 21.0, 20.9, 20.7, 20.7, 20.5 ppm; HRMS: *m/z* calcd for $C_{59}H_{74}N_2O_{26}Na^+$: 1249.4421 $[M+Na]^+$; found: 1249.4428.

Compound 14: Molecular sieves (AW-300, 4 Å, 2.0 g) were added to a solution of **12** (390 mg, 320 μmol) and **13** (424 mg, 320 μmol) in CH_2Cl_2 (10.0 mL). The suspension was stirred for 1 h at RT, after which TMSOTf (7.0 μL, 38 μmol) was added at 0 °C. Stirring at 0 °C was continued for 2 h (completion of the reaction was confirmed by TLC, EtOAc/MeOH 20:1). The reaction mixture was filtered through Celite and the removed molecular sieves were washed with $CHCl_3$. The combined filtrate and washings were extracted with $CHCl_3$, and the organic layer was washed with saturated aqueous $NaHCO_3$, and brine, dried (Na_2SO_4), and concentrated. The residue was purified by column chromatography on silica gel (EtOAc/MeOH 50:1) to give **14** (534 mg, 70%). $[\alpha]_D=-8.5°$ ($c=1.0$, $CHCl_3$); ^1H NMR (600 MHz, CD_3CN): $\delta=8.04$–7.23 (m, 20H; 4×Ph), 6.98–6.77 (2×d, 4H; Ar), 6.37 (d, $J_{2,NH}=9.6$ Hz, 1H; NHg), 6.07 (m, 3H; NHc, NHd, NHf), 5.40 (m, 1H; H-4d), 5.26 (m, 1H; H-4g), 5.18 (m, 4H; H-8f, H-7f, H-7c, H-3g), 5.08 (m, 2H; H-8c, H-2e), 5.00 (td, $J_{3eq,4}=4.8$ Hz, $J_{3ax,4}=J_{4,5}=11.0$ Hz, 1H; H-4f), 4.93 (td, $J_{3eq,4}=3.8$ Hz, $J_{3ax,4}=J_{4,5}=8.3$ Hz, 1H; H-4c), 4.86 (m, 3H; H-1g, H-1b, H-1e), 4.74 (d, 1H; PhCH_2), 4.62 (d, $J_{1,2}=8.2$ Hz, 1H; H-1d), 4.52 (m, 3H; H-3e, H-6′e, PhCH_2), 4.44 (q, 2H; PhCH_2), 4.34 (dd, $J_{gem}=11.7$ Hz, $J_{6,5}=6.8$ Hz, 1H; H-6e), 4.24 (m, 2H; H-3b, H-9′f), 4.14 (m, 1H; H-2g), 4.05–3.97 (m, 7H; H-9f, H-9c, H-9′c, H-5f, H-4b, H-3d, H-4e), 3.97–3.70 (m, 18H; 2×OMe, H-5d, H-6d, H-6′d, H-5g, H-6g, H-6g, H-2d, H-5e, H-5c, H-6f, H-6c, H-6b), 3.55 (m, 2H; H-5b, H-6′b), 3.42 (m, 1H; H-2b), 2.37 (dd, $J_{gem}=13.7$ Hz, $J_{3eq,4}=5.5$ Hz, 1H; H-3f$_{eq}$), 2.15–1.74 ppm (m, 54H; 17×Ac, H-3c$_{eq}$, H-3c$_{ax}$, H-3f$_{ax}$); ^{13}C NMR (150 MHz, CD_3CN): $\delta=171.3$, 171.3, 171.2, 171.2, 171.1, 171.0, 171.0, 170.8, 170.7, 170.7, 170.5, 170.4, 170.3, 169.5, 169.2, 166.8, 164.9, 156.2, 152.4, 139.8, 139.7, 134.2, 134.1, 131.1, 130.8, 130.6, 130.2, 129.5, 129.5, 129.2, 129.0, 128.4, 128.3, 119.0, 115.4, 103.2, 103.2, 102.2, 102.8, 100.5, 100.3, 79.4, 79.3, 79.1, 78.8, 75.8, 75.7, 74.2, 73.5, 72.6, 72.6, 72.5, 72.0, 71.8, 71.2, 71.2, 71.0, 70.9, 70.5, 70.4, 69.1, 68.6, 68.0, 67.5, 67.4, 64.8, 64.2, 62.8, 62.4, 62.4, 56.1, 53.9, 53.8, 52.1, 51.0, 49.3, 48.7, 35.8, 35.7, 23.3, 23.0, 23.0, 21.4, 21.3, 21.1, 21.0, 21.0, 20.9, 20.8, 20.7, 20.7 ppm; HRMS: *m/z* calcd for $C_{113}H_{138}N_4O_{53}Na^+$: 2421.8118 $[M+Na]^+$; found: 2421.8119.

Compound 15: $Pd(OH)_2$/C (20%, 412 mg) was added to a solution of compound **14** (412 mg, 170 μmol) in 1,4-dioxane (8.6 mL) and the suspension was stirred under a hydrogen stream for 16 h at RT (completion of the reaction was confirmed by TLC, EtOAc/MeOH 10:1). The reaction mixture was filtered through Celite and the removed molecular sieves were washed with $CHCl_3$. The combined filtrate and washings were concentrated and exposed to high vacuum. The residue was then treated with a solution of Bz_2O (156 mg, 690 μmol) and DMAP (11.0 mg, 86 μmol) in pyridine (6.0 mL) for 12 h at RT (completion of the reaction was confirmed by TLC, EtOAc/MeOH 10:1). The reaction mixture was then co-evaporated with toluene. The residue was extracted with $CHCl_3$ and the solution was washed with aqueous HCl (2M), H_2O, saturated aqueous $NaHCO_3$, and brine, dried (Na_2SO_4), and concentrated. The residue was purified by column chromatography on silica gel (EtOAc/MeOH 25:1) to give **15** (384 mg, 92%). $[\alpha]_D=+1.3°$ ($c=1.0$, $CHCl_3$); ^1H NMR (600 MHz, $CDCl_3$): $\delta=8.14$–7.42 (m, 20H; 4×Ph), 6.87–6.60 (2×d, 4H; Ar), 6.41 (d, $J_{NH,5}=6.9$ Hz, 1H; NHf), 5.67 (m, 2H; NHg, NHd), 5.56 (m, 1H; H-8f), 5.43 (m, 3H; H-8c, H-2e, H-4g), 5.34 (m, 1H; H-4d), 5.30 (near t, $J_{1,2}=J_{2,3}=7.6$ Hz, 1H; H-2b), 5.22 (m, 2H; H-3g, NHc), 5.14 (m, 3H; H-7f, H-7c, H-1e), 5.07 (d, $J_{1,2}=9.6$ Hz, 1H; H-1g), 4.97 (td, $J_{3eq,4}=3.4$ Hz, $J_{3ax,4}=J_{4,5}=8.2$ Hz, 1H; H-4f), 4.93 (d, $J_{1,2}=10.3$ Hz, 1H; H-1d), 4.80 (d, 1H; H-1b), 4.76 (td, $J_{3ax,4}=J_{4,5}=8.3$ Hz, $J_{3eq,4}=3.5$ Hz, 1H; H-4c), 4.62 (m, 2H; H-6′e, H-6′b), 4.49 (dd, $J_{3,4}=2.8$ Hz, $J_{2,3}=9.6$ Hz, 1H; H-3e), 4.41 (m, 2H; H-6e, H-6b), 4.32 (dd, $J_{3,4}=2.7$ Hz, $J_{2,3}=9.7$ Hz, 1H; H-3b), 4.16 (m, 2H; H-9′f, H-3d), 4.06 (m, 3H;

H-9′c, H-6d, H-6′d), 3.96–3.87 (m, 7H; H-9f, H-9c, H-5f, H-4b, H-5e, H-6g, H-5d), 3.86–3.75 (m, 10H; 2×OMe, H-5c, H-2d, H-5b, H-6g), 3.75–3.66 (m, 7H; OMe, H-4e, H-5g, H-6f, H-6c), 3.13 (m, 1H; H-2g), 2.82 (dd, J_{gem}=13.0 Hz, $J_{3eq,4}$=4.1 Hz, 1H; H-3f$_{eq}$), 2.42 (dd, J_{gem}=13.7 Hz, $J_{3eq,4}$=4.8 Hz, 1H; H-3c$_{eq}$), 2.16–1.62 ppm (m, 53H; 17×Ac, H-3c$_{ax}$, H-3f$_{ax}$); ^{13}C NMR (150 MHz, $CDCl_3$): δ=172.0, 171.1, 170.5, 170.3, 170.2, 170.1, 170.1, 170.0, 169.8, 169.7, 169.6, 168.1, 168.0, 167.6, 165.7, 165.6, 165.0, 164.3, 155.3, 151.3, 133.3, 133.0, 132.9, 132.2, 130.7, 129.9, 129.9, 129.8, 129.6, 129.4, 129.4, 128.6, 128.4, 128.3, 128.2, 119.2, 118.9, 114.2, 114.1, 100.9, 100.0, 98.2, 98.0, 97.3, 76.8, 76.8, 74.2, 73.2, 72.9, 72.7, 72.4, 71.9, 71.8, 71.7, 71.6, 70.6, 70.5, 70.3, 69.8, 69.7, 69.6, 68.7, 68.0, 67.2, 67.1, 66.9, 66.4, 66.3, 63.5, 63.1, 62.8, 62.2, 62.1, 61.3, 60.2, 55.3, 55.1, 52.8, 52.5, 52.0, 48.9, 38.5, 36.7, 36.2, 30.2, 29.4, 28.7, 23.5, 23.2, 22.9, 22.8, 22.7, 21.1, 20.9, 20.7, 20.5, 20.5, 20.2, 20.2, 19.9, 14.0, 13.9, 13.8, 10.7 ppm; HRMS: *m/z* calcd for $C_{113}H_{134}N_4O_{55}Na^+$: 2449.7710 $[M+Na]^+$; found: 2449.7709.

Compound 16: Diammonium cerium (IV) nitrate (1.1 g, 2.04 mmol) was added at 0 °C to a solution of **15** (495 mg, 200 μmol) in a mixture of MeCN (1.7 mL), toluene (1.5 mL), and H_2O (0.9 mL). The mixture was stirred at 0 °C for 20 min (completion of the reaction was confirmed by TLC, EtOAc/MeOH 10:1). The reaction mixture was diluted with Et_2O, and the solution was washed with saturated aqueous $NaHCO_3$ and brine, dried (Na_2SO_4), and concentrated. The residue was purified by column chromatography on silica gel ($CHCl_3$/MeOH 20:1) to give **16** (330 mg, 70%). HRMS: *m/z* calcd for $C_{106}H_{128}N_4O_{54}Na^+$: 2343.7295 $[M+Na]^+$; found: 2343.7291.

Compound 17: Trichloroacetonitrile (60 μL, 600 μmol) and DBU (0.9 μL, 5.9 μmol) were added at 0 °C to a solution of **16** (69 mg, 30 μmol) in CH_2Cl_2 (2.0 mL). The mixture was stirred for 10 h at RT (completion of the reaction was confirmed by TLC, $CHCl_3$/MeOH 15:1). The reaction mixture was concentrated and the residue was purified by column chromatography on silica gel ($CHCl_3$/MeOH 20:1) to give **17** (73 mg, quant). HRMS: *m/z* calcd for $C_{108}H_{128}Cl_3N_5O_{54}Na^+$: 2486.6386 $[M+Na]^+$; found: 2486.6387.

Compound 23: Compound **22** (29.0 mg, 58 μmol), DMAP (3.0 mg, 18 μmol), and EDC·HCl (12.0 mg, 64 μmol) were added at 0 °C to a solution of **21** (45.5 mg, 58 μmol) in CH_2Cl_2 (1.2 mL). The mixture was stirred for 5 h at RT (completion of the reaction was confirmed by TLC, toluene/EtOAc 2:1). The reaction mixture was diluted with $CHCl_3$, and the solution was washed with H_2O and brine, dried (Na_2SO_4), and concentrated. The residue was purified by column chromatography on silica gel (Et_2O/hexane 1:4) to give **23** (68 mg, 93%). $[\alpha]_D$=+4.9° (*c*=1.0, $CHCl_3$); ^{1}H NMR (400 MHz, $CDCl_3$): δ=8.00–7.20 (m, 10H; 2×Ph), 7.03–6.60 (2×d, 4H; Ar), 5.70 (m, $J_{NH,2}$=8.2 Hz, 2H; NH, H-5^{Cer}), 5.40 (t, 1H; H-4^{Cer}), 5.33 (m, 1H; H-3^{Cer}), 5.16 (t, $J_{1,2}$=10.1 Hz, $J_{2,3}$=9.2 Hz, 1H; H-2a), 4.73 (d, 1H; H-1a), 4.59 (s, 2H; ArCH_2), 4.39 (m, 2H; H-6a, H-6′a), 4.20 (m, 1H; H-2^{Cer}), 3.97 (d, $J_{4,OH}$=4.0 Hz, 1H; OH), 3.60 (m, 6H; OMe, H-4a, H-3a, H-1^{Cer}), 3.53 (m, 2H; H-5a, H-1′^{Cer}), 2.60 (s, 4H; OCOCH_2CH_2COO), 2,11 (t, 2H; NHCOCH_2), 1.96 (m, 2H; H-6^{Cer}, H-6′^{Cer}), 1.53 (m, 2H; NHCOCH$_2$CH_2), 1.21 (m, 50H; 25×CH_2), 0.83 (m, 15H; 5×CH_3), 0.01 ppm (m, 6H; Si(CH_3)$_2$); ^{13}C NMR (100 MHz, $CDCl_3$); δ=173.0, 172.5, 170.7, 165.1, 159.2, 136.7, 133.1, 132.8, 132.5, 130.0, 129.8, 129.7, 128.7, 128.4, 127.8, 124.4, 113.7, 86.4, 82.9, 77.9, 77.3, 74.4, 74.0, 72.0, 69.7, 63.2, 61.7, 60.4, 55.1, 51.8, 36.9, 32.4, 31.9, 29.7, 29.5, 29.5, 29.4, 29.3, 29.3, 29.2, 29.1, 29.0, 25.8, 22.7, 18.2, 14.1, −5.5, −5.6 ppm; HRMS: *m/z* calcd for $C_{73}H_{115}NO_{12}SSiNa^+$: 1280.7805 $[M+Na]^+$; found: 1280.7807.

Compound 24: AcOH (38.0 μL, 640 μmol) and TBAF (1.0 M solution in THF, 644.0 μL, 640 μmol) were added at 0 °C to a solution of **23** (270 mg, 220 μmol) in THF (2.2 mL). The mixture was stirred for 3 h at RT (completion of the reaction was confirmed by TLC, EtOAc/hexane 1:1). The reaction mixture was diluted with $CHCl_3$, and the solution was washed with saturated aqueous $NaHCO_3$ and brine, dried (Na_2SO_4), and concentrated. The residue was purified by column chromatography on silica gel (EtOAc/hexane 1:1.3) to give **24** (219 mg, 88%). $[\alpha]_D$=−6.1° (*c*=1.0, $CHCl_3$); ^{1}H NMR (600 MHz, $CDCl_3$): δ=8.03–7.24 (m, 10H; 2×Ph), 7.08–6.64 (2×d, 4H; Ar), 6.15 (d, $J_{NH,2}$=8.9 Hz, 1H; NH), 5.77 (m, 1H; H-5^{Cer}), 5.42 (m, 1H; H-4^{Cer}), 5.37 (t, 1H; H-3^{Cer}), 5.20 (dd, $J_{1,2}$=10.3 Hz, $J_{2,3}$=8.7 Hz, 1H; H-2a), 4.79 (d, 1H; H-1a), 4.64 (q, 2H; PhCH_2), 4.50 (dd, $J_{5,6}$=4.1 Hz, $J_{6,6'}$=12.4 Hz, 1H; H-6a), 4.37 (dd, 1H; H-6′a), 4.17 (m, 1H; H-2^{Cer}), 4.10 (d, $J_{4,OH}$=3.4 Hz, 1H; OHa), 3.71–3.57 (m, 8H; OMe, H-4a, H-3a, H-5a, H-1^{Cer}, H-1′^{Cer}), 3.16 (t, $J_{1,OH}$=$J_{1',OH}$=6.1 Hz, 1H; OH^{Cer}), 2.66 (m, 4H; OCOCH_2CH_2COO), 2,17 (m, 2H; NHCOCH_2), 2.00 (m, 2H; H-6^{Cer}, H-6′^{Cer}), 1.59 (m, 2H; NHCOCH$_2$CH_2), 1.31 (m, 50H; 25×CH_2), 0.88 ppm (t, 6H; 2×CH_3); ^{13}C NMR (150 MHz, $CDCl_3$): δ=173.7, 172.8, 171.5, 165.1, 159.3, 137.4, 133.2, 132.7, 132.5, 129.8, 129.8, 128.8, 128.4, 127.9, 124.4, 113.7, 86.4, 83.1, 77.7, 74.6, 74.5, 72.0, 69.5, 63.3, 61.6, 55.1, 52.9, 36.7, 32.3, 31.9, 29.7, 29.53, 29.47, 29.4, 29.3, 29.2, 29.1, 28.9, 25.7, 22.7, 14.1 ppm; HRMS: *m/z* calcd for $C_{67}H_{101}NO_{12}SNa^+$: 1166.6945 $[M+Na]^+$; found: 1166.6942.

Compound 25: Molecular sieves (4 Å, 85 mg) were added to a solution of **24** (85.0 mg, 740 μmol) in CH_2Cl_2 (15.0 mL). The suspension was stirred for 1 h at RT, after which DMTST (120.0 mg, 220 μmol) was added at 0 °C. Stirring was continued for 2 h at 0 °C (completion of the reaction was confirmed by TLC, toluene/EtOAc 1:1). The reaction mixture was filtered through Celite and the removed molecular sieves were washed with $CHCl_3$. The combined filtrate and washings were extracted with $CHCl_3$, and the organic layer was washed with saturated aqueous $NaHCO_3$ and H_2O, dried (Na_2SO_4), and concentrated. The residue was purified by column chromatography on silica gel ($CHCl_3$/MeOH 130:1) to give **25** (71 mg, 92%). $[\alpha]_D$=−29.2° (*c*=0.5, $CHCl_3$); ^{1}H NMR (600 MHz, $CDCl_3$): δ=8.03–7.45 (m, 5H; Ph), 7.19–6.78 (2×d, 4H; Ar), 5.78 (m, 1H; H-5^{Cer}), 5.70 (d, $J_{NH,2}$=8.9 Hz, 1H; NH), 5.26 (m, 2H; H-3^{Cer}, H-4^{Cer}), 5.17 (t, $J_{1,2}$=$J_{2,3}$=7.6 Hz, 1H; H-2a), 4.63 (2d, 2H; ArCH_2), 4.54 (d, 1H; H-1a), 4.41 (near t, $J_{5,6}$=8.9 Hz, $J_{6,6'}$=11.7 Hz, 1H; H-6a), 4.26 (m, 2H; H-6′a, H-2^{Cer}), 3.88 (dd, J_{gem}=9.6 Hz, $J_{1,2}$=3.4 Hz, 1H; H-1^{Cer}), 3.75 (s, 3H; OMe), 3.69–3.59 (m, 4H; H-3a, H-4a, H-5a, H-1′^{Cer}), 2.75–2.51 (m, 4H; OCOCH_2CH_2COO), 2.50 (d, $J_{4,OH}$=2.7 Hz, 1H; OH), 2.04 (t, 2H; NHCOCH_2), 1.95 (m, 2H; H-6^{Cer}, H-6′^{Cer}), 1.48 (m, 2H; NHCOCH$_2$CH_2), 1.26 (m, 50H; 25×CH_2), 0.88 ppm (t, 6H; 2×CH_3); ^{13}C NMR (150 MHz, $CDCl_3$): δ=172.7, 171.9, 170.6, 165.2, 159.5, 138.3, 133.4, 129.9, 129.7, 129.6, 128.5, 124.8, 114.0, 100.0, 82.0, 73.9, 73.7, 73.4, 72.9, 70.9, 66.7, 64.1, 55.2, 50.0, 36.7, 32.3, 31.9, 29.7, 29.7, 29.6, 29.6, 29.5, 29.4, 29.4, 29.3, 29.2, 28.9, 25.6, 22.7, 14.1 ppm; HRMS: *m/z* calcd for $C_{61}H_{95}NO_{12}Na^+$: 1056.6751 $[M+Na]^+$; found: 1056.6752.

Compound 27: Compound **26** (61 mg, 171 μmol), DMAP (2 mg, 17.1 μmol), and EDC·HCl (36 mg, 188 μmol) were added at 0 °C to a solution of **21** (133 mg, 171 μmol) in CH_2Cl_2 (3.4 mL). The mixture was stirred for 2 h at RT (completion of the reaction was confirmed by TLC, EtOAc/hexane 1:1). The reaction mixture was diluted with $CHCl_3$, and the solution was washed with aqueous HCl (2 M) and H_2O, dried (Na_2SO_4), and concentrated. The residue was purified by column chromatography on silica gel [i) EtOAc/hexane 1:5, ii) $CHCl_3$/MeOH 200:1] to give **27** (171 mg, 90%). $[\alpha]_D$=−20.4° (*c*=1.0, $CHCl_3$); ^{1}H NMR (500 MHz, $CDCl_3$): δ=7.49–7.29 (m, 5H; Ph), 5.74 (m, 2H; H-5^{Cer}, NH), 5.39 (m, 2H; H-3^{Cer}, H-4^{Cer}), 5.11 (t, $J_{2,3}$=$J_{3,4}$=9.5 Hz, 1H; H-3a), 4.94 (t, $J_{1,2}$=9.8 Hz, 1H; H-2a), 4.73 (d, 1H; H-1a), 4.65 (d, $J_{4,OH}$=4.6 Hz, 1H; OH), 4.48 (dd, $J_{5,6}$=3.5 Hz, J_{gem}=12.0 Hz, 1H; H-6a), 4.34 (dd, $J_{5,6'}$=2.0 Hz, 1H; H-6′a), 4.19 (m, 1H; H-2^{Cer}), 3.75 (m, 1H; H-4a), 3.66 (dd, $J_{1,2}$=2.9 Hz, J_{gem}=10.4 Hz, 1H; H-1^{Cer}), 3.56 (m, 2H; H-5a, H-1′^{Cer}), 2.71–2.57 (m, 4H; OCOCH_2CH_2COO), 2.15 (m, 2H; NHCOCH_2), 2.09 (s, 3H; Ac), 2.08 (s, 3H; Ac), 2.02 (m, 2H; H-6^{Cer}, H-6′^{Cer}), 1.57 (m, 2H; NHCOCH$_2$CH_2), 1.25 (m, 50H; 25×CH_2), 0.89 (m, 15H; *t*Bu, 2×CH_3), 0.04 ppm (m, 6H; Si(CH_3)$_2$); ^{13}C NMR (100 MHz, $CDCl_3$): δ=173.2, 172.4, 170.8, 170.4, 169.6, 136.8, 132.6, 132.3, 128.9, 128.1, 124.3, 85.9, 77.8, 77.3, 76.5, 73.9, 70.1, 67.7, 62.9, 61.7, 51.7, 36.9, 32.4, 31.9, 29.7, 29.5, 29.5, 29.4, 29.4, 29.3, 29.2, 29.1, 29.0, 25.8, 25.7, 22.7, 20.8, 18.2, 14.1, −5.6, −5.7 ppm; HRMS: *m/z* calcd for $C_{62}H_{107}NO_{12}SSiNa^+$: 1140.7176 $[M+Na]^+$; found: 1140.7175.

Compound 28: Molecular sieves (4 Å, 130 mg) were added to a solution of **27** (62 mg, 55.5 μmol) in $(CH_2Cl)_2$ (11.0 mL). The suspension was stirred for 1 h at RT, after which DMTST (90 mg, 167 μmol) was added. Stirring was continued for 1 h at 40 °C (completion of the reaction was confirmed by TLC, acetone/hexane 1:2). TFA (5.5 mL) was added at 0 °C to the reaction mixture. Stirring was continued for 2 h at 0 °C. The reaction mixture was filtered through Celite and the removed molecular sieves were washed with $CHCl_3$. The combined filtrate and washings

were extracted with $CHCl_3$, and the organic layer was washed with saturated aqueous Na_2CO_3, dried (Na_2SO_4), and concentrated. The residue was purified by column chromatography on silica gel (acetone/hexane 1:5) to give **28** (36 mg, 72%). $[\alpha]_D=-16.1°$ ($c=0.7$, $CHCl_3$); ^1H NMR (500 MHz, $CDCl_3$): $\delta=5.80$ (m, 1H; H-5^{Cer}), 5.72 (d, $J_{2,NH}=9.8$ Hz, 1H; NH), 5.30 (m, 2H; H-3^{Cer}, H-4^{Cer}), 4.95 (t, $J_{2,3}=J_{3,4}=8.3$ Hz, 1H; H-3a), 4.88 (t, $J_{1,2}=7.5$ Hz, 1H; H-2a), 4.47 (m, 2H; H-1a, H-6a), 4.32 (m, 1H; H-2^{Cer}), 4.27 (dd, $J_{5,6'}=2.3$ Hz, $J_{gem}=12.0$ Hz, 1H; H-6′a), 3.87 (dd, $J_{1,2}=4.9$ Hz, $J_{gem}=10.0$ Hz, 1H; H-1^{Cer}), 3.77 (dd, $J_{1',2}=4.0$ Hz, 1H; H-1′^{Cer}), 3.62 (m, 2H; H-4a, H-5a), 2.83 (d, $J_{4,OH}=4.6$ Hz, 1H; OH), 2.73–2.56 (m, 4H; $OCOCH_2CH_2COO$), 2.16 (m, 2H; $NHCOCH_2$), 2.12 (s, 3H; Ac), 2.05 (s, 3H; Ac), 1.96 (m, 2H; H-6^{Cer}, H-6′^{Cer}), 1.59 (m, 2H; $NHCOCH_2CH_2$), 1.25 (m, 50H; $25\times CH_2$), 0.88 ppm ($2\times$t, 6H; $2\times CH_3$); ^{13}C NMR (125 MHz, $CDCl_3$): $\delta=172.8$, 172.0, 171.9, 170.4, 169.4, 138.0, 124.5, 99.6, 76.6, 73.5, 71.2, 70.4, 66.4, 63.7, 50.0, 36.8, 32.3, 31.9, 29.7, 29.7, 29.5, 29.5, 29.4, 29.2, 28.9, 25.7, 22.7, 20.9, 20.8, 14.1 ppm; HRMS: m/z calcd for $C_{50}H_{87}NO_{12}Na^+$: 916.6121 $[M+Na]^+$; found: 916.6120.

Compound 30: Molecular sieves (AW-300, 4 Å, 200 mg) were added to a solution of **25** (25.0 mg, 24 μmol) and **13** (32.0 mg, 24 μmol) in $CHCl_3$ (800 μL). The suspension was stirred for 1 h at RT, after which TMSOTf (0.4 μL, 1.9 μmol) was added at 0 °C. Stirring was continued for 2 h at 0 °C (completion of the reaction was confirmed by TLC, toluene/EtOAc/MeOH 5:5:1). The reaction mixture was filtered through Celite and the removed molecular sieves were washed with $CHCl_3$. The combined filtrate and washings were extracted with $CHCl_3$, and the organic layer was washed with saturated aqueous $NaHCO_3$ and brine, dried (Na_2SO_4), and concentrated. The residue was purified by column chromatography on silica gel (toluene/EtOAc/MeOH 10:10:1) to give **30** (37 mg, 70%). $[\alpha]_D=+1.8°$ ($c=0.8$, $CHCl_3$); ^1H NMR (600 MHz, $CDCl_3$): $\delta=8.10$–7.43 (m, 15H; $3\times$Ph), 7.20–6.70 ($2\times$d, 4H; Ar), 6.04 (d, $J_{NH,2}=8.2$ Hz, 1H; NHd), 5.73 (m, 1H; H-5^{Cer}), 5.58 (d, $J_{NH,2}=9.6$ Hz, 1H; NH^{Cer}), 5.40 (m, 3H; H-3d, H-2b, H-8c), 5.34 (m, 1H; H-4d), 5.26–5.11 (m, 5H; H-7c, NHc, H-2a, H-3^{Cer}, H-4^{Cer}), 5.07 (m, 1H; H-4c), 5.02 (d, $J_{1,2}=8.3$ Hz, 1H; H-1d), 4.84 (d, $J_{gem}=11.0$ Hz, 1H; $ArCH_2$), 4.82 (d, $J_{1,2}=8.2$ Hz, 1H; H-1b), 4.69 (dd, $J_{gem}=11.7$ Hz, $J_{5,6}=6.2$ Hz, 1H; H-6b), 4.64 (d, 1H; $ArCH_2$), 4.45 (d, $J_{1,2}=6.9$ Hz, 1H; H-1a), 4.33 (dd, $J_{2,3}=10.3$ Hz, $J_{3,4}=2.8$ Hz, 1H; H-3b), 4.25–4.03 (m, 9H; H-2d, H-6d, H-6′d, H-5d, H-6′a, H-9c, H-9′c, H-6′b, H-2^{Cer}), 4.02–3.74 (m, 11H; OMe, H-4b, H-5b, H-6a, H-5a, H-4a, H-5c, H-6c, H-1^{Cer}), 3.64 (s, 3H; OMe), 3.54 (near t, 1H; H-3a), 3.50 (dd, $J_{gem}=9.6$ Hz, $J_{1',2}=3.4$ Hz, 1H; H-1′^{Cer}), 2.55–2.35 (m, 4H; $OCOCH_2CH_2COO$), 2.25 (dd, $J_{gem}=13.1$ Hz, $J_{3eq,4}=4.8$ Hz, 1H; H-3c$_{eq}$), 2.15–1.84 (m, 32H; $9\times$Ac, H-3c$_{ax}$, H-6^{Cer}, H-6′^{Cer}, $NHCOCH_2$), 1.45 (m, 2H; $NHCOCH_2CH_2$), 1.25 (m, 50H; $25\times CH_2$), 0.88 ppm (t, 6H; $2\times CH_3$); ^{13}C NMR (150 MHz, $CDCl_3$): $\delta=172.6$, 171.1, 170.8, 170.5, 170.3, 170.2, 169.9, 169.7, 168.1, 165.9, 165.1, 164.3, 158.9, 138.2, 133.3, 133.1, 130.5, 130.1, 129.9, 129.7, 129.6, 129.5, 129.4, 129.2, 128.4, 124.9, 113.5, 101.5, 101.2, 99.5, 98.6, 80.5, 79.0, 76.5, 74.1, 73.9, 73.3, 73.0, 72.3, 72.0, 70.9, 70.7, 70.1, 68.7, 67.4, 67.0, 66.6, 66.5, 63.5, 63.1, 62.1, 61.4, 55.0, 53.2, 51.3, 49.9, 49.3, 36.6, 36.4, 35.9, 32.2, 31.9, 29.7, 29.7, 29.5, 29.5, 29.4, 29.3, 29.3, 28.9, 25.5, 23.3, 23.2, 22.7, 21.1, 20.8, 20.7, 20.6, 20.5, 20.4, 14.1 ppm; HRMS: m/z calcd for $C_{115}H_{159}N_3O_{39}Na^+$: 2229.0448 $[M+Na]^+$; found: 2229.0448.

Compound 31: Molecular sieves (AW-300, 4 Å, 300 mg) were added to a solution of **28** (40 mg, 44.8 μmol) and **13** (60 mg, 44.8 μmol) in $CHCl_3$ (448 μL). The suspension was stirred for 1 h at RT, after which TMSOTf (0.8 μL, 4.48 μmol) was added at 0 °C. Stirring was continued for 1 h at 0 °C (completion of the reaction was confirmed by TLC, acetone/hexane 1:1). TFA (224 μL) was added to the reaction mixture. Stirring was continued for 2 h at 0 °C. The reaction mixture was filtered through Celite and the removed molecular sieves were washed with $CHCl_3$. The combined filtrate and washings were extracted with $CHCl_3$, and the organic layer was washed with saturated aqueous Na_2CO_3, dried (Na_2SO_4), and concentrated. The residue was purified by column chromatography on silica gel (acetone/hexane 2:3) to give **31** (45 mg, 48%). $[\alpha]_D=-13.7°$ ($c=0.7$, $CHCl_3$); ^1H NMR (600 MHz, $CDCl_3$): $\delta=8.11$–7.43 (m, 10H; $2\times$Ph), 6.42 (d, $J_{2,NH}=7.6$ Hz, 1H; NHd), 5.75 (m, 2H; H-5^{Cer}, H-3d), 5.67 (d, $J_{2,NH}=9.6$ Hz, 1H; NH^{Cer}), 5.53 (m, 1H; H-8c), 5.33 (m, 2H; H-4d, H-2b), 5.24 (m, 3H; H-3^{Cer}, H-4^{Cer}, H-7c), 5.14 (m, 3H; H-1d, H-3a, NHc), 4.88 (m, 1H; H-4c), 4.82 (t, $J_{1,2}=J_{2,3}=7.6$ Hz, 1H; H-2a), 4.73 (d, $J_{1,2}=7.6$ Hz, 1H; H-1b), 4.67 (dd, $J_{5,6}=6.6$ Hz, $J_{gem}=11.3$ Hz, 1H; H-6b), 4.42 (dd, $J_{2,3}=10.3$ Hz, $J_{3,4}=2.8$ Hz, 1H; H-3b), 4.33 (m, 2H; H-1a, H-6′b), 4.27 (m, 3H; H-6a, H-9c, H-2^{Cer}), 4.14 (near d, 1H; H-6′a), 4.03–3.95 (m, 4H; H-9′c, H-6d, H-6′d, H-5d), 3.89 (m, 2H; H-5b, H-5c), 3.83–3.78 (m, 5H; H-4b, H-6c, $COOCH_3$), 3.74–3.67 (m, 4H; H-4a, H-2d, H-1^{Cer}, H-1′^{Cer}), 3.49 (near t, 1H; H-5a), 2.61–2.48 (m, 5H; $OCOCH_2CH_2COO$, H-3c$_{eq}$), 2.16–1.82 ($11\times$s, 33H; $11\times$Ac), 2.13–1.84 (m, 5H; H-3c$_{ax}$, H-6^{Cer}, H-6′^{Cer}, $NHCOCH_2$), 1.57 (m, 2H; $NHCOCH_2CH_2$), 1.23 (m, 50H; $25\times CH_2$), 0.88 ppm ($2\times$t, 6H; $2\times CH_3$); ^{13}C NMR (150 MHz, $CDCl_3$): $\delta=172.7$, 171.3, 170.6, 170.3, 170.3, 170.2, 170.2, 170.1, 169.9, 169.4, 168.2, 165.8, 164.6, 137.6, 133.4, 133.3, 130.2, 129.8, 129.5, 129.2, 128.6, 128.5, 124.5, 100.7, 100.1, 99.3, 98.0, 76.7, 74.3, 73.4, 73.3, 73.1, 72.2, 72.0, 71.8, 71.7, 70.5, 70.1, 69.4, 68.7, 67.3, 66.9, 66.5, 66.3, 63.0, 62.7, 62.3, 61.4, 53.0, 52.4, 50.0, 49.1, 36.7, 36.4, 32.2, 31.9, 29.7, 29.6, 29.5, 29.4, 29.3, 29.3, 29.2, 28.8, 25.6, 23.4, 23.1, 22.6, 21.2, 20.8, 20.7, 20.6, 20.4, 20.3, 14.1 ppm; HRMS: m/z calcd for $C_{104}H_{151}N_3O_{39}Na^+$: 2088.9818 $[M+Na]^+$; found: 2088.9817.

Compound 32: Molecular sieves (AW-300, 4 Å, 200 mg) were added to a solution of **29** (39 mg, 41.1 μmol) and **13** (55 mg, 41.1 μmol) in $CHCl_3$ (820 μL). The suspension was stirred for 30 min at RT, after which TMSOTf (0.8 μL, 4.11 μmol) was added at 0 °C. Stirring was continued for 1 h at 0 °C (completion of the reaction was confirmed by TLC, acetone/hexane 1:1). The reaction mixture was filtered through Celite and the removed molecular sieves were washed with $CHCl_3$. The combined filtrate and washings were extracted with $CHCl_3$, and the organic layer was washed with saturated aqueous $NaHCO_3$, dried (Na_2SO_4), and concentrated. The residue was purified by column chromatography on silica gel (acetone/hexane 1:1) to give **32** (24 mg, 28%). $[\alpha]_D=-3.5°$ ($c=1.0$, $CHCl_3$); ^1H NMR (600 MHz, $CDCl_3$): $\delta=8.09$–7.39 (m, 15H; $3\times$Ph), 6.40 (d, 1H; $J_{2,NH}=7.5$ Hz, NHd), 5.85–5.79 (m, 2H; H-3d, H-5^{Cer}), 5.70 (d, $J_{2,NH}=9.6$ Hz, 1H; NH^{Cer}), 5.52–5.41 (m, 3H; H-8c, H-3^{Cer}, H-4^{Cer}), 5.35 (d, $J_{3,4}=3.5$ Hz, 1H; H-4d), 5.29–5.24 (m, 2H; H-2b, H-7c), 5.21 (d, $J_{1,2}=8.3$ Hz, 1H; H-1d), 5.13 (t, $J_{2,3}=J_{3,4}=9.3$ Hz, 1H; H-3a), 4.99 (d, $J_{5,NH}=9.6$ Hz, 1H; NHc), 4.89–4.82 (m, 2H; H-2a, H-4c), 4.70 (d, $J_{1,2}=8.2$ Hz, 1H; H-1b), 4.65 (dd, $J_{5,6}=6.2$ Hz, $J_{gem}=11.0$ Hz, 1H; H-6b), 4.42 (m, 1H; H-2^{Cer}), 4.39 (dd, $J_{2,3}=10.3$ Hz, $J_{3,4}=2.1$ Hz, 1H; H-3b), 4.35–4.32 (m, 2H; H-1a, H-6′b), 4.31 (dd, $J_{8,9}=2.4$ Hz, $J_{gem}=12.7$ Hz, 1H; H-9c), 4.09–3.90 (m, 7H; H-6a, H-6′a, H-9′c, H-5d, H-6d, H-6′d, H-1^{Cer}), 3.88–3.81 (m, 3H; H-4a, H-5b, H-5c), 3.78 (s, 3H; $COOCH_3$), 3.77–3.75 (m, 2H; H-4b, H-6c), 3.59–3.53 (m, 2H; H-2d, H-1′^{Cer}), 3.35 (m, 1H; H-5a), 2.61 (dd, $J_{3eq,4}=4.9$ Hz, $J_{gem}=13.0$ Hz, 1H; H-3c$_{eq}$), 2.15, 2.14, and 2.13 ($3\times$s, 9H; $3\times$Ac), 2.12–2.08 (m, 4H; $NHCOCH_2$), 2.06–1.98 (m, 17H; H-6^{Cer}, H-6′^{Cer}, 5 Ac), 1.96 and 1.88 ($2\times$s, 6H; $2\times$Ac), 1.82–1.78 (m, 7H; H-3c$_{ax}$, 2 Ac), 1.57 (m, 2H; $NHCOCH_2CH_2$), 1.30–1.22 (m, 50H; $25\times CH_2$), 0.88 ppm ($2\times$t, $J=6.6$ Hz, 6H; $2\times CH_2CH_3$); ^{13}C NMR (150 MHz, $CDCl_3$): $\delta=172.7$, 171.5, 170.7, 170.4, 170.4, 170.2, 170.2, 170.1, 170.1, 169.8, 169.6, 168.3, 165.9, 165.2, 164.6, 137.4, 133.5, 133.3, 130.0, 130.2, 130.2, 129.7, 129.6, 129.5, 129.2, 128.7, 128.5, 128.3, 124.6, 100.5, 100.2, 99.6, 97.8, 74.5, 74.2, 73.5, 73.4, 72.7, 72.6, 71.9, 71.6, 71.4, 70.6, 70.1, 69.0, 68.8, 67.3, 66.9, 66.2, 62.8, 61.9, 61.8, 61.4, 52.9, 52.8, 50.7, 49.2, 36.8, 36.6, 32.3, 31.9, 29.7, 29.7, 29.6, 29.5, 29.5, 29.4, 29.3, 29.2, 28.9, 25.7, 23.4, 23.1, 22.7, 21.3, 20.9, 20.7, 20.7, 20.7, 20.5, 20.4, 20.3, 14.1 ppm; HRMS: m/z calcd for $\frac{1}{2}(C_{104}H_{151}N_3O_{39})+Na^+$: 1088.0011 $[\frac{1}{2}M+Na]^+$; found: 1088.0014.

Compound 33: Molecular sieves (AW-300, 4 Å, 100 mg) were added to a solution of **25** (20.0 mg, 20 μmol) and **17** (48.0 mg, 20 μmol) in $CHCl_3$ (0.96 mL). The suspension was stirred for 1 h at RT, after which TMSOTf (0.7 μL, 3.9 μmol) was added at 0 °C. Stirring was continued for 2 h at RT (completion of the reaction was confirmed by TLC, $CHCl_3$/EtOAc/MeOH 3:3:1). The reaction mixture was filtered through Celite and the removed molecular sieves were washed with $CHCl_3$. The combined filtrate and washings were extracted with $CHCl_3$, and the organic layer was washed with saturated aqueous $NaHCO_3$ and brine, dried (Na_2SO_4), and concentrated. The residue was purified by column chromatography on silica gel ($CHCl_3$/EtOAc/MeOH 8:8:1) to give **33** (39 mg, 60%). $[\alpha]_D=+3.5°$ ($c=0.2$, $CHCl_3$); ^1H NMR (600 MHz, $CDCl_3$): $\delta=8.15$–7.35 (m, 25H; $5\times$Ph), 7.10–6.64 ($2\times$d, 4H; Ar), 6.41 (d, $J_{NH,5}=7.6$ Hz, 1H; NHf), 5.65 (m, 5H; H-5^{Cer}, NH^{Cer}, H-8f, NHg, NHd), 5.41 (m, 2H; H-4d, H-8c), 5.33 (m, 1H; H-4g), 5.29 (m, 2H; H-2b, H-2e), 5.19 (m, 4H; H-3^{Cer}, H-

4^{Cer}, H-7f, H-7c), 5.10 (m, 4H; NHc, H-1d, H-2a, H-3g), 4.95 (m, 3H; H-1e, H-1g, H-4f), 4.77 (m, 3H; H-1b, H-4c, ArCH_2), 4.62 (m, 2H; H-6e, H-6b), 4.55 (d, 1H; ArCH_2), 4.46 (dd, $J_{3,4}$=2.8 Hz, $J_{3,2}$=9.6 Hz, 1H; H-3e), 4.39 (m, 2H; H-1a, H-6'b), 4.29 (m, 2H; H-3b, H-9'f), 4.15 (m, 4H; H-6a, H-6'a, H-9c, H-2^{Cer}), 4.06–4.01 (m, 4H; H-6d, H-3d, H-9f, H-9'c), 4.01–3.86 (m, 4H; H-6'd, H-6g, H-6'e, H-4b), 3.85–3.68 (m, 20H; H-5b, H-5e, H-2d, H-5f, H-5c, H-3a, H-4a, H-5a, H-6g, H-6f, H-6c, H-4e, H-5g, H-5d, 2×OMe), 3.60 (s, 3H; OMe), 3.52 (m, 1H; H-1^{Cer}), 3.48 (m, 1H; H-$1'^{Cer}$), 3.22 (m, 1H; H-2g), 2.72 (dd, J_{gem}=13.7 Hz, $J_{3eq,4}$=4.8 Hz, 1H; H-3f_{eq}), 2.60–2.44 (m, 4H; OCOCH_2CH_2COO), 2.37 (m, 1H; H-3c_{eq}), 2.20–1.52 (m, 57H; 17×Ac, NHCOCH_2, H-3f_{ax}, H-3c_{ax}, H-6^{Cer}, H-$6'^{Cer}$), 1.42 (m, 2H; NHCOCH$_2$CH_2), 1.25 (m, 50H; 25×CH_2), 0.86 ppm (t, 6H; 2×CH_3); ^{13}C NMR (150 MHz, $CDCl_3$): δ=172.7, 171.1, 170.8, 170.8, 170.7, 170.6, 170.5, 170.4, 170.3, 170.2, 170.2, 170.1, 170.0, 169.8, 168.3, 168.2, 165.9, 165.6, 165.1, 164.4, 158.9, 133.3, 133.2, 132.9, 130.4, 130.3, 130.0, 129.9, 129.7, 129.7, 129.5, 129.3, 129.2, 129.0, 128.8, 128.7, 128.5, 128.3, 128.2, 113.5, 101.1, 100.2, 99.5, 98.1, 97.7, 80.9, 78.5, 73.9, 73.7, 73.5, 73.3, 73.2, 72.6, 72.3, 72.0, 71.9, 71.0, 70.9, 70.6, 70.0, 69.8, 68.9, 68.8, 67.3, 66.9, 66.5, 66.5, 63.2, 63.1, 63.0, 62.6, 62.2, 61.4, 55.0, 54.9, 53.0, 52.7, 49.9, 49.3, 37.4, 37.4, 37.1, 36.7, 36.5, 36.3, 34.4, 32.7, 32.2, 31.9, 31.2, 30.4, 30.3, 30.1, 30.0, 29.9, 29.7, 29.7, 29.5, 29.5, 29.4, 29.3, 29.3, 28.8, 27.4, 27.1, 25.5, 24.8, 24.5, 23.4, 23.2, 23.1, 23.1, 23.0, 22.7, 21.3, 21.2, 20.8, 20.7, 20.7, 20.4, 20.4, 20,2, 20.1, 19.7, 14.4, 14.1, 11.4 ppm; HRMS: *m/z* calcd for $C_{167}H_{221}N_5O_{65}Na^+$: 3359.4032 $[M+Na]^+$; found: 3359.4039.

Compound 34: Trifluoroacetic acid (180 μL) was added at 0 °C to a solution of **33** (18.0 mg, 54 μmol) in CH_2Cl_2 (360 μL). The mixture was stirred for 50 min at 0 °C (completion of the reaction was confirmed by TLC, $CHCl_3$/EtOAc/MeOH 3:3:1). The reaction mixture was diluted with $CHCl_3$, and the solution was washed with ice-cooled H_2O, saturated aqueous $NaHCO_3$, and brine, dried (Na_2SO_4), and concentrated. The residue was purified by column chromatography on silica gel ($CHCl_3$/EtOAc/MeOH 8:8:1) to give **34** (17 mg, quant). $[\alpha]_D$=−17.0° (*c*=0.2, $CHCl_3$); ^{1}H NMR (600 MHz, $CDCl_3$): δ=8.17–7.26 (m, 25H; 5×Ph), 6.47 (d, $J_{NH,5}$=7.6 Hz, 1H; NHf), 5.75–5.58 (m, 5H; H-5^{Cer}, NH^{Cer}, H-8f, NHg, NHd), 5.42 (m, 2H; H-4d, H-8c), 5.38–5.27 (m, 3H; H-4g, H-2b, H-2e), 5.25–5.01 (m, 8H; H-3^{Cer}, H-4^{Cer}, H-7f, H-7c, NHc, H-1d, H-2a, H-3g), 5.01–4.90 (m, 3H; H-1e, H-1g, H-4f), 4.85–4.72 (m, 2H; H-1b, H-4c), 4.70–4.62 (m, 2H; H-6e, H-6b), 4.52 (m, 1H; H-3e), 4.41 (m, 4H; H-1a, H-6'b, H-3b, H-9f), 4.31–4.12 (m, 4H; H-6a, H-6'a, H-9c, H-2^{Cer}), 4.10–3.85 (m, 8H; H-6d, H-3d, H-9'f, H-9'c, H-6'd, H-6g, H-6'e, H-4b), 3.85–3.68 (m, 20H; H-5b, H-5e, H-2d, H-5f, H-5c, H-3a, H-4a, H-5a, H-6g, H-6f, H-6c, H-4e, H-5g, H-5d, 2×OMe), 3.65–3.47 (m, 2H; H-1^{Cer}, H-$1'^{Cer}$), 3.21 (m, 1H; H-2g), 2.70 (dd, J_{gem}=13.7 Hz, $J_{3eq,4}$=4.8 Hz, 1H; H-3f_{eq}), 2.60–2.44 (m, 4H; OCOCH_2CH_2COO), 2.40 (m, 1H; H-3c_{eq}), 2.20–1.41 (m, 59H; 17×Ac, NHCOCH_2, H-3f_{ax}, H-3c_{ax}, H-6^{Cer}, H-$6'^{Cer}$, NHCOCH$_2$CH_2), 1.29 (m, 50H; 25×CH_2), 0.86 ppm (t, 6H; 2×CH_3); ^{13}C NMR (150 MHz, $CDCl_3$): δ=172.7, 171.9, 171.3, 170.9, 170.8, 170.5, 170.4, 170.2, 170.0, 169.9, 169.7, 168.2, 166.2, 165.9, 165.4, 164.9, 164.4, 137.9, 133.3, 133.1, 130.9, 130.2, 130.1, 129.8, 129.8, 129.7, 129.6, 129.5, 129.2, 128.8, 128.6, 128.5, 128.4, 124.7, 101.3, 101.1, 100.3, 99.7, 98.7, 98.2, 97.8, 82.7, 78.1, 78.0, 77.7, 77.3, 73.5, 73.2, 73.1, 72.9, 72.7, 72.5, 72.0, 71.9, 71.6, 70.9, 70.7, 70.5, 70.4, 70.1, 70.0, 69.6, 68.8, 67.3, 66.9, 66.6, 66.5, 64.1, 63.2, 63.0, 62.6, 62.2, 61.7, 61.4, 53.1, 52.8, 52.2, 50.0, 49.2, 49.1, 37.4, 37.1, 36.7, 36.6, 36.4, 34.4, 32.7, 32.2, 31.9, 31.7, 30.8, 30.4, 30.0, 29.7, 29.5, 29.5, 29.4, 29.3, 29.2, 28.8, 27.1, 26.7, 25.5, 23.4, 23.1, 23.1, 22.7, 21.4, 21.2, 20.8, 20.8, 20.7, 20.5, 20.4, 20.4, 20.3, 19.7, 14.1 ppm; HRMS: *m/z* calcd for $C_{159}H_{213}N_5O_{64}Na^+$: 3239.3460 $[M+Na]^+$; found: 3239.3464.

Ganglioside GalNAc-GD1a (1): A catalytic amount of sodium methoxide (28% in MeOH) was added at RT to a solution of **34** (13.0 mg, 4.0 μmol) in a mixture of MeOH (200 μL) and THF (200 μL). The mixture was stirred for 5 days at RT. Water (10 μL) was added and stirring was continued for 2 days at RT (completion of the reaction was confirmed by TLC, $CHCl_3$/MeOH/H_2O 5:4:1), the reaction mixture was neutralized with Dowex-50 (H^+), the mixture was filtered through cotton, and removed resin was washed with mixed solvent ($CHCl_3$/MeOH 1:1). The combined filtrate and washings were concentrated. The residue was purified by column chromatography on silica gel ($CHCl_3$/MeOH/H_2O 5:4:0.5) to give **1** (7 mg, 88%). $[\alpha]_D$=−3.5° (*c*=0.1, MeOH); ^{1}H NMR (600 MHz, $CDCl_3$/CD_3OD 1:1): δ=5.60 (m, 1H; H-5^{Cer}), 5.37 (m, 1H; H-4^{Cer}), 2.69 (m, 2H; H-3c_{eq}, H-3f_{eq}), 2.10 (t, 2H; NHCOCH_2), 1.95 (s, 14H; H-6^{Cer}, H-$6'^{Cer}$, 4×Ac), 1.82 (m, 2H; H-3c_{ax}, H-3f_{ax}), 1.50 (m, 2H; NHCOCH$_2$CH_2), 1.25 (m, 50H; 25×CH_2), 0.81 ppm (t, 6H; 2×CH_3); ^{13}C NMR (150 MHz, $CDCl_3$): δ=177.9, 175.9, 175.6, 175.6, 175.1, 174.6, 170.5, 135.6, 131.6, 104.9, 104.4, 104.2, 103.2, 101.3, 101.3, 101.1, 88.9, 84.7, 84.1, 81.4, 79.5, 79.2, 76.4, 76.2, 76.1, 75.9, 75.8, 75.1, 74.1, 73.9, 73.8, 73.5, 72.9, 71.6, 71.0, 70.6, 70.5, 69.9, 69.7, 69.0, 68.8, 65.5, 65.3, 63.0, 62.9, 61.7, 60.5, 57.5, 57.3, 57.2, 57.1, 56.0, 54.5, 53.8, 50.3, 50.1, 49.9, 49.6, 49.4, 49.3, 49.1, 48.9, 48.8, 48.7, 48.6, 48.1, 48.0, 47.9, 43.3, 38.8, 37.4, 36.9, 36.1, 33.5, 33.1, 31.0, 30.9, 30.8, 30.7, 30.7, 30.6, 30.5, 30.4, 27.2, 24.0, 23.8, 23.7, 23.6, 23.4, 22.6, 17.4, 16.3, 14.9, 14.7, 14.5 ppm; HRMS: *m/z* calcd for $C_{92}H_{161}N_5O_{44}^{2-}$:1019.0815 $[1/2M-2H]^{2-}$; found: 1019.0815.

Acknowledgements

This work was financially supported by MEXT of Japan (WPI program and grant-in-aid for Scientific Research to M.K., No. 1701007 and No. 22380067). We thank Kiyoko Ito for technical assistance.

[1] H. J. Willison, N. Yuki, *Brain* **2002**, *125*, 2591–2625.
[2] A. Uncini, N. Yuki, *Expert. Rev. Neurother.* **2009**, *9*, 869–884.
[3] a) S. Kusunoki, A. Chiba, K. Kon, S. Ando, K. Arisawa, A. Tate, I. Kanazawa, *Ann. Neurol.* **1994**, *35*, 570–576; b) S. Kusunoki, M. Iwamori, A. Chiba, S. Hitoshi, M. Arita, I. Kanazawa, *Neurology* **1996**, *47*, 237–242; c) N. Yuki, T. Taki, S. Handa, *J. Neuroimmunol.* **1996**, *71*, 155–161; d) N. Yuki, Y. Tagawa, F. Irie, Y. Hirabayashi, S. Handa, *J. Neuroimmunol.* **1997**, *74*, 30–34.
[4] Ganglioside GalNAc-GD1a was first isolated from human brain; L. Svennerholm, J.-E. Mansson, Y. T. Li, *J. Biol. Chem.* **1973**, *248*, 740–742.
[5] K. Fujikawa, T. Nohara, A. Imamura, H. Ando, H. Ishida, M. Kiso, *Tetrahedron Lett.* **2010**, *51*, 1126–1130.
[6] A. Imamura, H. Ando, H. Ishida, M. Kiso, *J. Org. Chem.* **2009**, *74*, 3009–3023.
[7] a) T. Fuse, H. Ando, A. Imamura, S. Sawada, H. Ishida, M. Kiso, T. Ando, S.-C. Li, Y.-T. Li, *Glycoconjugate J.* **2006**, *23*, 329–343; b) A. Imamura, H. Ando, H. Ishida, M. Kiso, *Org. Lett.* **2005**, *7*, 4415–4418.
[8] H. Ando, Y. Koike, H. Ishida, M. Kiso, *Tetrahedron Lett.* **2003**, *44*, 6883–6886.
[9] J. C. Castro-Palomino, G. Ritter, S. R. Fortunato, S. Reinhardt, L. J. Old, R. R. Schmidt, *Angew. Chem.* **1997**, *109*, 2081–2085; *Angew. Chem. Int. Ed. Engl.* **1997**, *36*, 1998–2001.
[10] a) P. Konradsson, U. E. Udodong, B. Fraser-Reid, *Tetrahedron Lett.* **1990**, *31*, 4313–4316; b) P. Konradsson, D. R. Mootoo, R. E. McDevitt, B. Fraser-Reid, *J. Chem. Soc. Chem. Commun.* **1990**, 270–272; c) G. H. Veeneman, S. H. Van Leeuwen, J. H. Van Boom, *Tetrahedron Lett.* **1990**, *31*, 1331–1334.
[11] T. Komori, A. Imamura, H. Ando, H. Ishida, M. Kiso, *Carbohydr. Res.* **2009**, *344*, 1453–1463.
[12] a) R. R. Schmidt, J. Michel, *Angew. Chem.* **1980**, *92*, 763–764; *Angew. Chem. Int. Ed. Engl.* **1980**, *19*, 731–732; b) R. R. Schmidt, *Angew. Chem.* **1986**, *98*, 213–236; *Angew. Chem. Int. Ed. Engl.* **1986**, *25*, 212–235.
[13] Original paper on intramolecular glycosylation exploiting succinyl tethering: T. Ziegler; R. Lau, *Tetrahedron Lett.* **1995**, *36*, 1417–1420; R. Lau, *Tetrahedron Lett.* **1995**, *36*, 1417–1420.
[14] Experimental details for the synthesis of this compound were reported in the Supporting Information.
[15] K. Fujikawa, A. Imamura, H. Ishida, M. Kiso, *Carbohydr. Res.* **2008**, *343*, 2729–2734.
[16] P. Fügedi, P. J. Garegg, *Carbohydr. Res.* **1986**, *149*, C9-C12.
[17] B. Yu, J. Xie, S. Deng, Y. Hui, *J. Am. Chem. Soc.* **1999**, *121*, 12196–12197.
[18] Reports on intermolecular glycosylation of trialkylsilylated hydroxy group; a) T. Mukaiyama, T. Shimpuku, T. Takashima, S. Kobayashi,

Chem. Lett. **1989**, 145–148; b) E. M. Nashed, C. P. J. Glaudemans, *J. Org. Chem.* **1989**, *54*, 6116–6118; c) T. Mukaiyama, T. Takashima, M. Katsurada, H. Aizawa, *Chem. Lett.* **1991**, 533–536.

[19] a) M. Karplus, *J. Am. Chem. Soc.* **1963**, *85*, 2870–2871; b) Y. Nishida, H. Ohrui, H. Meguro, *Tetrahedron Lett.* **1984**, *25*, 1575–1578; c) Y. Nishida, H. Hori, H. Ohrui, H. Meguro, *Carbohydr. Res.* **1987**, *170*, 106–111; d) Y. Nishida, H. Hori, H. Ohrui, H. Meguro, *J. Carbohydr. Chem.* **1988**, *7*, 239–250.

[20] S. Wolfe, *Acc. Chem. Res.* **1972**, *5*, 102–111.

Received: November 22, 2010
Published online: April 5, 2011

Reprinted from

APPLIED PHYSICS EXPRESS

Micropatterning of Polydiacetylene Nanoparticle Monolayer Based on Ultraviolet or Electron Beam Polymerization

Daisuke Tanaka, Hisashi Karube, Masayuki Shimojo, and Kotaro Kajikawa

Appl. Phys. Express **4** (2011) 121604

Applied Physics Express 4 (2011) 121604
DOI: 10.1143/APEX.4.121604

Micropatterning of Polydiacetylene Nanoparticle Monolayer Based on Ultraviolet or Electron Beam Polymerization

Daisuke Tanaka, Hisashi Karube, Masayuki Shimojo,[1] and Kotaro Kajikawa*

Interdisciplinary Graduate School of Science and Engineering, Tokyo Institute of Technology, Yokohama 226-8502, Japan
[1]*Materials Science and Engineering, Shibaura Institute of Technology, Koto, Tokyo 135-8548, Japan*

Received November 10, 2011; accepted November 16, 2011; published online December 6, 2011

A simple fabrication method is reported to obtain patterned polydiacetylene (PDA) nanoparticle (NP) monolayers, on the basis of polymerization of diacetylene NPs by UV light or electron beam (EB) irradiation. The UV patterning can be made within a resolution of 1.1 μm, using a mesh copper grid as a mask. The EB irradiation also brings about the polymerization, and patterned PDA NP monolayers were formed; however, the resolution of the patterning was lower than expected (~2.5 μm), even using a narrow EB. Electron scattering, heating or defocusing will be the cause of the lower resolution. © 2011 The Japan Society of Applied Physics

Polydiacetylene (PDA) is a π-conjugated polymer that has attractive optical properties, such as large nonlinear optical activity,[1–3] ultrashort response time,[4,5] and fluorescence.[6,7] Many applications require thin PDA films patterned in a desired shape. For example, a waveguide of PDA was fabricated using deep-UV lithography using an organosilicone photoresist film.[8] A PDA self-assembled monolayer (SAM) was used as a UV photoresist for the electrochemical etching of a thin gold film.[9] The photopatterning of a PDA/polymer complex film spin-coated on a substrate was reported, in which the PDA structure is stabilized by hydrogen bonding between the PDA and the matrix polymer.[6]

In this letter, we show a simple method to obtain micropatterned PDA nanoparticle (NP) monolayers. First, a diacetylene (DA) NP monolayer is formed on a silicone substrate, by immersion of an amino silane SAM-coated substrate in a colloidal solution of DA NPs. Then, the deposited DA NPs are polymerized by UV or electron beam (EB) irradiation in a desired form. The PDA NPs cleave to the substrate and are barely removed by rinsing with acetone, while the DA NPs on the substrate are reasonably soluble in it. Reflection absorption spectroscopy certainly confirms that the residual materials on the substrate are PDA NPs.

The DA material used in this study was 1,6-bis(*N*-carbazolyl)-2,4-hexadiyne (DCHD), purchased from Wako Pure Chemical. The DA NPs were prepared by the reprecipitation method proposed by Nakanishi and colleagues.[10,11] 300 μL of a DCHD acetone solution at 5 mM was injected into 10 mL of ultrapure water at 50 °C and the solution was vigorously stirred for 10 min. A silicone substrate was prepared by exposure to an ethanolic mixture solution of *N*-(2-aminoethyl)-3-aminopropyltrimethoxysilane (SILA-ACE; Chisso S320) (1.1% v/v) and acetic acid (5% v/v), at room temperature for 10 min. The substrate was rinsed with ethanol, followed by annealing at 120 °C for silanization for 30 min. Then, we have an organosilane SAM having an amino group, which acts as an adhesion layer between the silicone substrate and the NPs. After that, the substrate was immersed in the DA NP solution to immobilize the DA NPs on the substrate for 2 h, followed by rinsing with ultrapure water. According to the SEM images, the obtained DA NPs are rectangular parallelepipeds whose edges are 50–300 nm.[11]

*E-mail address: kajikawa@ep.titech.ac.jp

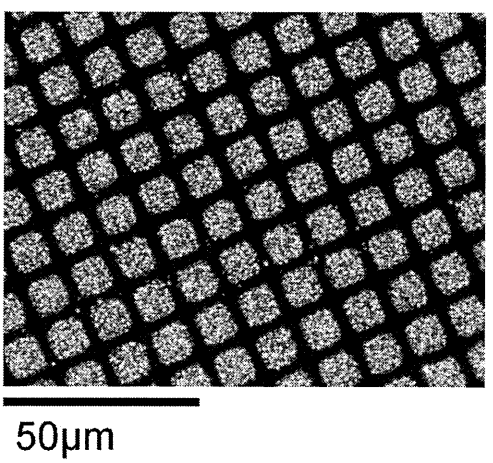

Fig. 1. Dark-field optical microscopy image of the UV-patterned PDA NP monolayers using a mesh grid.

Polymerization of the DA was carried out by UV exposure of the substrate using a low pressure Hg lamp of 40 W (Sen Lights SUV40GS-6) having two major lines at 186 and 254 nm. The substrate was placed below the lamp with a distance of 8 cm. The exposure time was 15 min. A copper mesh electron microscopy grid was attached to the DA NP-coated substrate used as a photomask. After the UV exposure, the substrate was rinsed with acetone. The EB polymerization was carried out using a scanning electron microscope (SEM; JEOL JIB-4500). The EB was produced with an acceleration voltage of 10 kV. The typical EB exposure time was 1 s. After the EB polymerization, the substrate was rinsed with acetone.

Reflection absorption spectroscopy was carried out with an MCPD-3000 spectrometer (Otsuka Electronics). Light from a halogen lamp was guided and focused with a lens on the sample surface at normal incidence using a Y-type optical fiber, and reflected light was conveyed to the spectrometer through the same optical fiber.

Figure 1 shows the dark-field optical microscopy image of the patterned DA NP on the silicone substrate. The square patches of PDA NPs are clearly observed and they are obviously separated. There are few NPs in the gaps between the squires, indicating that the DA NPs are completely rinsed off from the substrate, whereas the PDA NPs stay densely in the squares. As determined from the image, the mean side